



# The Evolution of SlyA/RovA Transcription Factors from Repressors to Countersilencers in *Enterobacteriaceae*

W. Ryan Will,<sup>a</sup> Peter Brzovic,<sup>b</sup> Isolde Le Trong,<sup>c</sup> Ronald E. Stenkamp,<sup>b,c</sup> Matthew B. Lawrenz,<sup>d</sup> Joyce E. Karlinsky,<sup>e</sup> William W. Navarre,<sup>e\*</sup> Kara Main-Hester,<sup>e</sup> Virginia L. Miller,<sup>f,g</sup> Stephen J. Libby,<sup>a</sup>  Ferric C. Fang<sup>a,e</sup>

<sup>a</sup>Department of Laboratory Medicine, University of Washington, Seattle, Washington, USA

<sup>b</sup>Department of Biochemistry, University of Washington, Seattle, Washington, USA

<sup>c</sup>Department of Biological Structure, University of Washington, Seattle, Washington, USA

<sup>d</sup>Department of Microbiology and Immunology and the Center for Predictive Medicine for Biodefense and Emerging Infectious Diseases, University of Louisville School of Medicine, Louisville, Kentucky, USA

<sup>e</sup>Department of Microbiology, University of Washington, Seattle, Washington, USA

<sup>f</sup>Department of Microbiology and Immunology, University of North Carolina School of Medicine, Chapel Hill, North Carolina, USA

<sup>g</sup>Department of Genetics, University of North Carolina School of Medicine, Chapel Hill, North Carolina, USA

**ABSTRACT** Gene duplication and subsequent evolutionary divergence have allowed conserved proteins to develop unique roles. The MarR family of transcription factors (TFs) has undergone extensive duplication and diversification in bacteria, where they act as environmentally responsive repressors of genes encoding efflux pumps that confer resistance to xenobiotics, including many antimicrobial agents. We have performed structural, functional, and genetic analyses of representative members of the SlyA/RovA lineage of MarR TFs, which retain some ancestral functions, including repression of their own expression and that of divergently transcribed multidrug efflux pumps, as well as allosteric inhibition by aromatic carboxylate compounds. However, SlyA and RovA have acquired the ability to countersilence horizontally acquired genes, which has greatly facilitated the evolution of *Enterobacteriaceae* by horizontal gene transfer. SlyA/RovA TFs in different species have independently evolved novel regulatory circuits to provide the enhanced levels of expression required for their new role. Moreover, in contrast to MarR, SlyA is not responsive to copper. These observations demonstrate the ability of TFs to acquire new functions as a result of evolutionary divergence of both *cis*-regulatory sequences and in *trans* interactions with modulatory ligands.

**IMPORTANCE** Bacteria primarily evolve via horizontal gene transfer, acquiring new traits such as virulence and antibiotic resistance in single transfer events. However, newly acquired genes must be integrated into existing regulatory networks to allow appropriate expression in new hosts. This is accommodated in part by the opposing mechanisms of xenogeneic silencing and countersilencing. An understanding of these mechanisms is necessary to understand the relationship between gene regulation and bacterial evolution. Here we examine the functional evolution of an important lineage of countersilencers belonging to the ancient MarR family of classical transcriptional repressors. We show that although members of the SlyA lineage retain some ancestral features associated with the MarR family, their *cis*-regulatory sequences have evolved significantly to support their new function. Understanding the mechanistic requirements for countersilencing is critical to understanding the pathoadaptation of emerging pathogens and also has practical applications in synthetic biology.

**KEYWORDS** SlyA, countersilencing, evolution, gene regulation, transcription factors

**Citation** Will WR, Brzovic P, Le Trong I, Stenkamp RE, Lawrenz MB, Karlinsky JE, Navarre WW, Main-Hester K, Miller VL, Libby SJ, Fang FC. 2019. The evolution of SlyA/RovA transcription factors from repressors to countersilencers in *Enterobacteriaceae*. mBio 10:e00009-19. <https://doi.org/10.1128/mBio.00009-19>.

**Editor** Nancy E. Freitag, University of Illinois at Chicago

**Copyright** © 2019 Will et al. This is an open-access article distributed under the terms of the [Creative Commons Attribution 4.0 International license](https://creativecommons.org/licenses/by/4.0/).

Address correspondence to Ferric C. Fang, [fcfang@uw.edu](mailto:fcfang@uw.edu).

\* Present address: William W. Navarre, University of Toronto, Toronto, Ontario, Canada.

S.J.L. and F.C.F. contributed equally to this paper.

**Received** 2 January 2019

**Accepted** 29 January 2019

**Published** 5 March 2019

As organisms adapt to new or changing environments, their regulatory networks must evolve to ensure that individual genes are appropriately expressed in response to environmental signals (1). An important mechanism for the evolution of conserved essential proteins, including transcription factors (TFs), is gene duplication, which allows the subsequent diversification of gene and protein families and the development of new functions (2). More than 50% of bacterial genes are believed to have descended from original duplication events (3–5), providing a broad foundation from which bacteria can evolve complex and adaptive traits.

The MarR family is an ancient family of TFs, predating the divergence of archaea and bacteria (6). It has undergone extensive gene duplication events, with recent estimates suggesting that bacteria encode an average of seven MarR TFs per genome (7). MarR TFs typically function as environmentally responsive repressors of genes encoding efflux pumps that export xenobiotics, including many antimicrobial agents, and are defined by the presence of a winged helix-turn-helix (wHTH) DNA-binding domain (8). The prototypical MarR protein of *Escherichia coli* represses a single operon, *marRAB*, which encodes a transcriptional activator (MarA) required for the expression of the AcrAB efflux pump, which in turn confers resistance to  $\beta$ -lactams, quinolones, and tetracyclines (9–11). MarR is allosterically regulated by many small molecules, in particular small aromatic carboxylate compounds such as salicylate, which induce a structural change that reduces the affinity of MarR for DNA (10, 12–14) and derepresses the expression of its cognate promoters. A recent study suggests that MarR can also be inhibited by intracellular copper ( $\text{Cu}^{2+}$ ), which oxidizes a conserved cysteine residue at position 80, promoting the formation of disulfide bonds between MarR dimers and causing individual dimers to dissociate from DNA (15). Free copper is thought to be liberated from membrane-bound cytoplasmic proteins during envelope stress induced by antimicrobial agents. Dimerization of MarR TFs is required for DNA binding, as it allows these proteins to recognize palindromic sequences via the  $\alpha 4$  recognition helix, which makes sequence-specific contacts with the major groove, while the wing makes sequence-independent contacts via the minor groove (16).

A duplication event producing the SlyA lineage of MarR TFs most likely resulted from an ancient horizontal gene transfer event or from intragenomic recombination of a MarR family TF prior to the divergence of the *Enterobacteriaceae*. SlyA has been best characterized in *Salmonella enterica* serovar Typhimurium, where it serves primarily to upregulate virulence genes (17–19). Although this contrasts with the classical repressive role of MarR TFs, work in our and other laboratories has demonstrated that SlyA positively regulates genes by a countersilencing mechanism, in which repression of AT-rich promoters by the histone-like nucleoid-associated protein H-NS is relieved by SlyA (17, 20). SlyA cooperatively remodels the H-NS–DNA complex in concert with the response regulator PhoP (20, 21), which is activated by conditions found within phagosomal compartments, including low  $\text{Mg}^{2+}$  (22), acidic pH (23), and cationic antimicrobial peptides (24). SlyA orthologs, represented by Hor, Rap, and RovA in *Pectobacterium* (*Erwinia*), *Serratia*, and *Yersinia*, respectively (25), are conserved in nearly every species of *Enterobacteriaceae*, even including endosymbionts such as *Sodalis glossinidius* (26), which have undergone extensive gene loss and degenerative evolution (27). This high degree of conservation suggests that the SlyA lineage occupies an essential role in the regulatory network organization of *Enterobacteriaceae*. Although conclusive mechanistic evidence to demonstrate that other SlyA orthologs function as countersilencers has not yet been obtained, existing evidence is strongly suggestive of countersilencing, as several are known to upregulate horizontally acquired traits, which are generally repressed by H-NS, in a number of species, including *Yersinia* spp. (28–30), *Dickeya dadantii* (31), *Pectobacterium carotovorum* (25), and *Shigella flexneri* (32).

TFs can evolve in two ways: in *cis*, through their promoters and associated regulatory elements, both transcriptional and posttranscriptional, altering expression patterns to respond to different environmental and physiological stimuli, and in *trans*, affecting their interactions with cognate binding sites, other proteins, and regulatory ligands. We sought to understand the evolutionary transition of the SlyA/RovA TF lineage from the

ancestral function of MarR family TFs as environmentally responsive and dedicated repressors of small regulons to countersilencers of extensive networks of horizontally acquired genes, with a particular focus on in *cis* changes in gene expression and in *trans* changes in modulation by inhibitory ligands. Structural and comparative analyses of representative members of the SlyA lineage were performed to identify the evolutionary changes that allowed SlyA to adopt its new role. Here we show that SlyA has retained an ability to undergo conformational changes in response to aromatic carboxylates, regulate gene expression in an environmentally responsive manner, and repress the expression of a linked drug efflux system. However, SlyA/RovA lineage genes have undergone extensive evolution in *cis* to support the higher levels of expression that are required for countersilencing. Finally, we show that linked efflux pumps are not conserved in some *Enterobacteriaceae*, even though SlyA/RovA TFs have been evolutionarily retained, suggesting that these regulators have been conserved not due to their primordial role in regulating antimicrobial resistance but rather as a consequence of their countersilencing function, which is essential to maintain the regulated expression of horizontally-acquired genes in *Enterobacteriaceae*.

## RESULTS

**Salicylate-mediated inhibition of SlyA activity.** As environmentally-responsive repressors whose conformation and regulatory actions are modulated by small aromatic carboxylates (12, 14), MarR family TFs are inhibited by salicylate *in vitro* (12). In their structural analyses of SlyA-DNA interactions, Dolan et al. (33) inferred from our structural data (see below) that salicylate might regulate SlyA. Using electrophoretic mobility shift assays, they demonstrated that salicylate inhibits DNA binding by SlyA. To confirm that this influences the function of SlyA as a transcriptional regulator, we performed *in vitro* transcription assays (IVT assays) of *slyA* and the divergently transcribed *ydhIJK* efflux pump operon. Supercoiled plasmid DNA containing the *slyA-ydhIJK* region was incubated with RNA polymerase (RNAP) and increasing SlyA concentrations in the presence or absence of salicylate. SlyA repressed *slyA* transcription approximately 5.3-fold, while *ydhI* transcription was inhibited ~19-fold (Fig. 1A and B). The addition of 2 mM sodium salicylate reduced SlyA-mediated repression to 2.8-fold and 3.2-fold, respectively, indicating that the sensitivity to aromatic carboxylates observed in classical MarR TFs has been retained by SlyA. IVT assays of the SlyA-upregulated gene *pagC* confirmed that SlyA does not function as a classical activator (Fig. 1C).

We then confirmed that the *ydhIJK* operon encodes a functional antimicrobial efflux pump by growing wild-type and *slyA*, *ydhIJK*, and *slyA ydhIJK* mutant strains in the presence of an aromatic carboxylate with antimicrobial activity, fusaric acid (Fig. 1D). Both the *ydhIJK* and *slyA ydhIJK* mutant strains exhibited delayed growth in the presence of fusaric acid relative to the wild-type strain, suggesting that *ydhIJK* confers fusaric acid resistance in wild-type *S. Typhimurium*. Conversely, *slyA* mutants exhibit improved growth in the presence of fusaric acid, as predicted when *ydhIJK* is derepressed. Collectively, these observations indicate that the *S. Typhimurium* SlyA TF has retained ancestral functions characteristic of the MarR family.

To determine whether salicylate inhibits SlyA-mediated countersilencing as well as repression, expression of the countersilenced *pagC* gene was measured by qRT-PCR in the presence or absence of 2 mM sodium salicylate (Fig. 1E). Wild-type cultures grown in salicylate phenocopied a *slyA* mutant strain, with a >14-fold reduction in *pagC* expression, indicating that salicylate is a general allosteric inhibitor of SlyA function, most likely inducing a structural change that reduces affinity for DNA as described in other MarR TFs (8, 10). Unexpectedly, SlyA retained an ability to interact with DNA upstream of the *ydhI* promoter even in the presence of salicylate (see Fig. S1 in the supplemental material), but this interaction may represent nonspecific interactions with the wing domain, as salicylate inhibited SlyA interaction with a 12-bp DNA region that is highly homologous (75% identity) to the consensus high-affinity binding site (19, 34, 35), centered near the -35 position of the *ydhI* transcription start site (TSS).

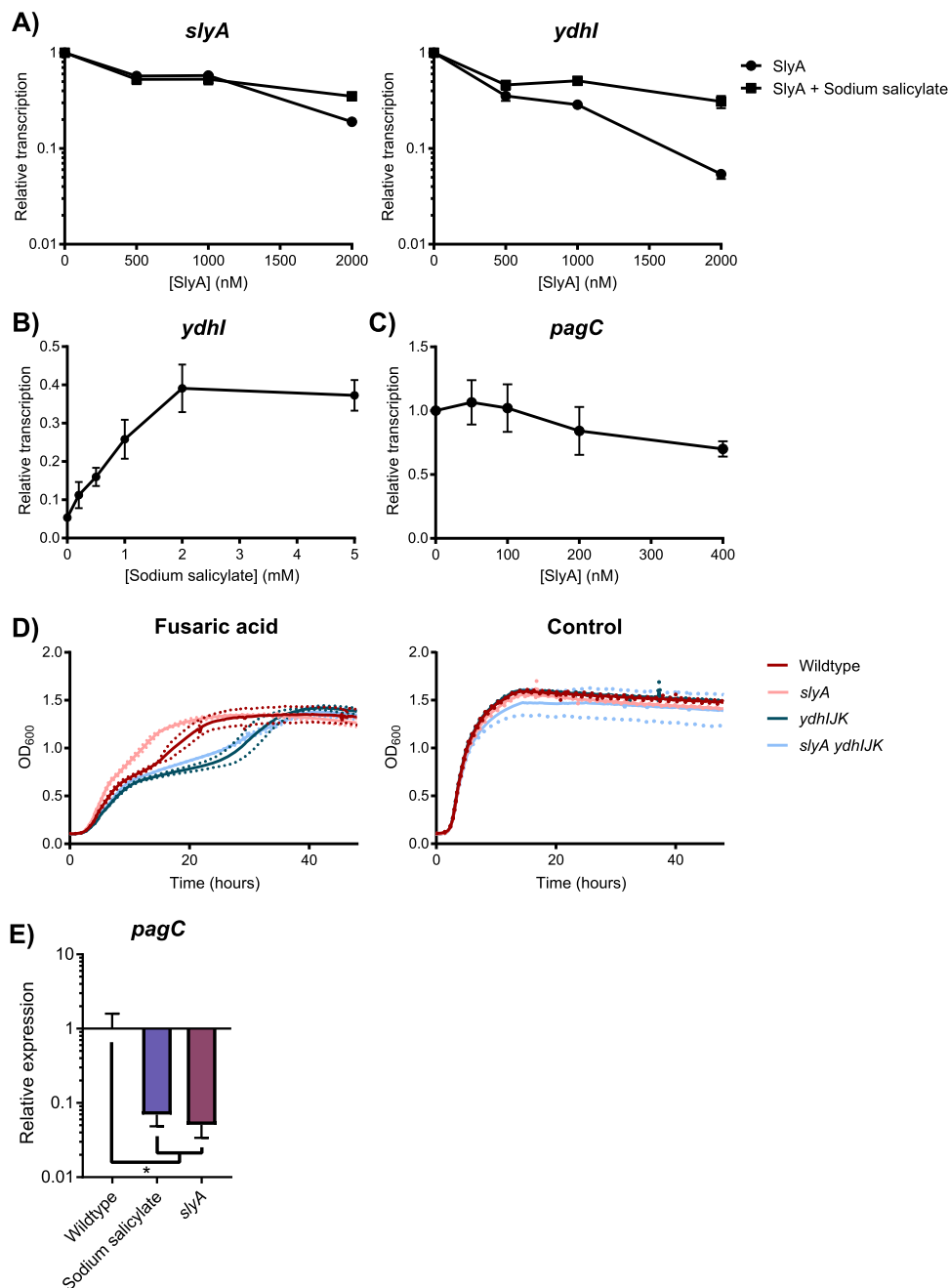


**FIG 1** SlyA retains the ancestral functions of MarR family TFs. To determine whether SlyA is an autorepressor like other members of the MarR family, *in vitro* transcription (IVT) assays were performed on supercoiled template DNA containing *slyA* and the divergently expressed *ydhI* gene in the presence of increasing SlyA concentrations (A). Reactions were performed with or without 2 mM sodium salicylate to determine whether SlyA is inhibited by small aromatic carboxylate compounds like other MarR TFs. To determine whether SlyA exhibits a dose-dependent response to salicylate, IVT assays were performed on *ydhI* in the presence of 2  $\mu$ M SlyA and increasing concentrations of sodium salicylate (B). To confirm that SlyA does not function as an activator at upregulated targets, IVT assays of the model SlyA target gene, *pagC*, were performed in the presence of increasing concentrations of SlyA (C). All IVT data represent the mean  $\pm$  SEM ( $n \geq 3$ ). Wild-type, *slyA*, *ydhIJK*, and *slyA ydhIJK* cultures were grown in the presence of 30  $\mu$ g/ml fusaric acid, and cell density (OD<sub>600</sub>) was measured over time to determine if *ydhIJK* encodes a functional antimicrobial efflux pump (D). Data represent the mean (solid line) from three independent experiments, each consisting of three replicates. Dashed lines represent the SD. The control plot represents the growth curve of each strain in the absence of fusaric acid. To determine whether salicylate also inhibits SlyA countersilencing activity, *pagC* transcripts were quantified by qRT-PCR from early-stationary-phase (OD<sub>600</sub>  $\approx$  2.0) cultures in minimal N-medium containing 10  $\mu$ M MgCl<sub>2</sub> in the presence or absence of 2 mM sodium salicylate (E). Transcript levels are normalized to *rpoD*, and data represent the mean  $\pm$  SD ( $n \geq 3$ ). Asterisk indicates  $P = 0.05$ .

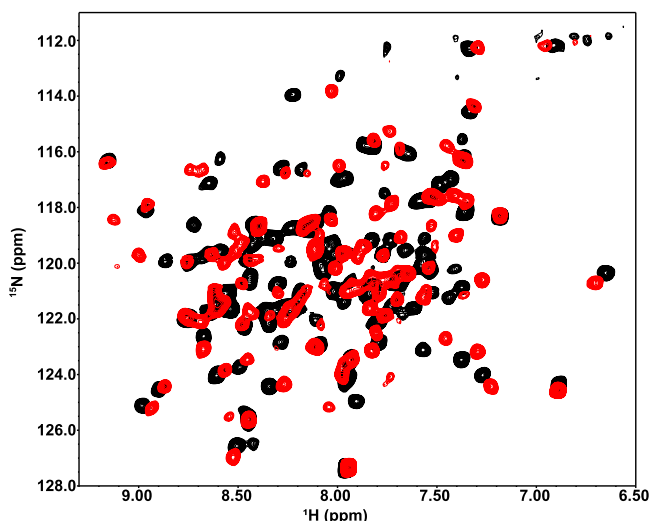


**FIG 2** SlyA undergoes significant structural alterations upon salicylate binding. To assess salicylate-induced SlyA structural changes,  $^1\text{H},^{15}\text{N}$ -TROSY NMR spectroscopy was performed on 0.3 mM uniformly labeled  $^{15}\text{N}$ -SlyA in the absence (black) or presence (red) of 2 mM sodium salicylate. (Results of differential DNA footprinting analysis [DDFA] of the SlyA-DNA interaction and ligand binding analyses are shown in Fig. S1.)

To determine whether salicylate-mediated inhibition correlates with structural changes in SlyA,  $^1\text{H},^{15}\text{N}$  transverse relaxation-optimized spectroscopy (TROSY) NMR spectra of *S. Typhimurium* SlyA in the presence or absence of salicylate were collected. The apo-SlyA spectrum is well dispersed (Fig. 2), with  $\sim 85\%$  of the expected resonances observed. However, wide variation among individual resonances with respect to peak width and intensity may signify (i) weak nonspecific interactions between SlyA dimers, (ii) various rates of exchange of amide protons with solvent, or (iii) conformational exchange. Previous studies of MarR found that apo-MarR is also highly disordered (8), suggesting that the observed spectral characteristics of apo-SlyA can be ascribed to the presence of multiple conformational states in solution. Addition of salicylate to SlyA induces chemical shift perturbations throughout the spectrum, and nearly 90% of expected resonances are now observed. The large-scale changes in chemical shifts show that backbone amides throughout the protein are stabilized in a different environment relative to apo-SlyA. These observations are consistent with ligand binding to SlyA dimers inducing global structural changes, likely stabilizing a single protein conformation in solution, a conformation that is no longer able to interact with specific high-affinity DNA binding sites. The affinity of the SlyA-ligand interaction was determined via the quenching of intrinsic tryptophan fluorescence in the presence of increasing concentrations of benzoate, an analogous small aromatic carboxylate compound (Fig. S1). Benzoate induces chemical shift perturbations similar to those observed in response to salicylate but does not cause inner filter effects that interfere with fluorescence measurement, as there is relatively little overlap between the UV spectra of benzoate and SlyA, in contrast to salicylate. Although this assay was not able to differentiate between multiple SlyA-benzoate interactions, the  $K_D$  (equilibrium dissociation constant) of the SlyA-benzoate interaction was determined to be  $\sim 40 \mu\text{M}$ , which is similar to the previously determined affinities for EmrR/MprA and HucR (1 to 10  $\mu\text{M}$ ) and significantly stronger than that of the MarR-salicylate interaction (0.5 to 1 mM) (13, 36).

**Crystal structure of salicylate-SlyA.** To further analyze the mechanism of allosteric inhibition of SlyA, the structure of the salicylate-SlyA cocrystal was determined. Studies by other groups have previously determined the structure of apo-SlyA and the SlyA bound to DNA (33), demonstrating that SlyA is similar in overall structure to other MarR proteins, consisting of six alpha helices (Fig. 3A). Helices  $\alpha 1$ ,  $\alpha 5$ , and  $\alpha 6$  make up the

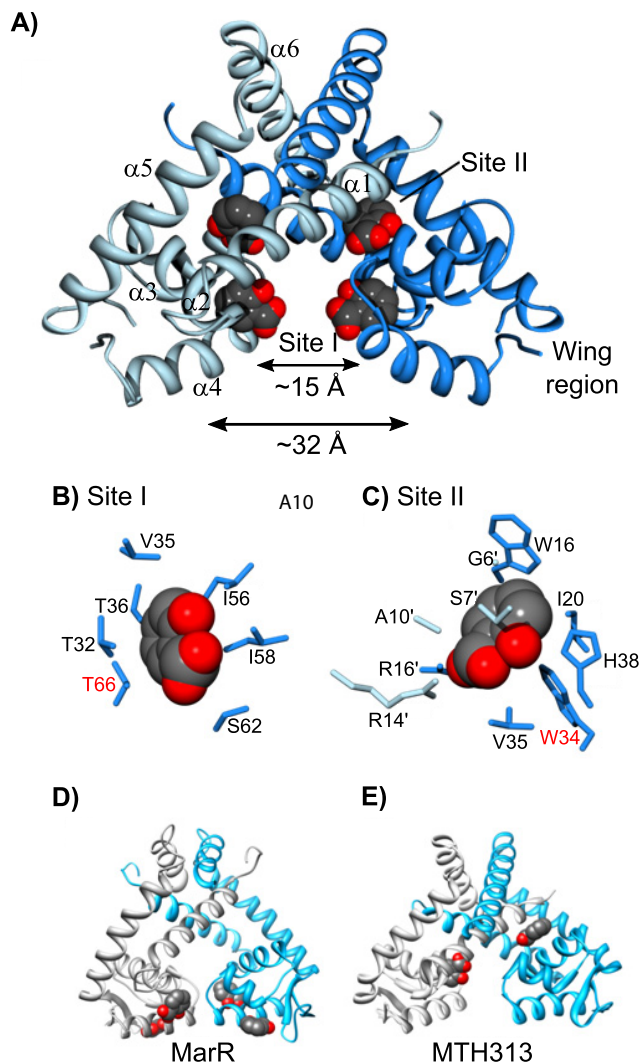


**FIG 3** Structure of the SlyA dimer bound to salicylate. The crystal structure of the SlyA dimer with salicylate bound at sites I and II was determined at a resolution of 2.3 Å (A). Residues involved in coordinating bound salicylates are shown for sites I (B) and II (C). Residues required for salicylate-mediated inhibition of SlyA (Fig. 4) are highlighted in red. The structures of salicylate-bound MarR (D) (PDB entry 1JGS) and MTH313 (E) (PDB entry 3BPX) dimers are shown for comparison.

dimerization domain, while  $\alpha 3$  and  $\alpha 4$ , along with the wing region between  $\alpha 4$  and  $\alpha 5$ , comprise the wHTH DNA-binding domain. These two domains are separated by  $\alpha 2$ . Dolan et al. (33) previously observed that the two recognition helices of the apo-SlyA dimer are only  $\sim 15 \text{ \AA}$  apart, in a closed conformation. During interaction with a high-affinity binding site, the helices move a significant distance to accommodate the 32-Å distance between major grooves.

SlyA formed large crystals in the presence of 75 mM sodium salicylate. However, we were unable to obtain usable crystals of apo-SlyA. Diffraction data set and refinement statistics are summarized in Table S1. The two SlyA molecules in the asymmetric unit form two different SlyA dimers in this crystal form. Space group symmetry operations generate the other subunit in each dimer. The dimers are very similar in structure, and further discussion will focus on the dimer formed by polypeptide chain A. We were unable to observe electron density for the tips of the wings, so these regions are absent from our structural model. Difference electron density maps ( $|F_o| - |F_c|$ ) identified two salicylate molecules bound per SlyA monomer at sites referred to as site I and site II (Fig. 3A to C). Salicylate molecules interact with these sites via hydrophobic interactions

with their aromatic rings, while the carboxylate and hydroxyl groups are positioned to interact with the solvent. Site I is composed of residues from  $\alpha 2$ ,  $\alpha 3$ , and  $\alpha 4$ , as well as 158 in the loop between  $\alpha 3$  and  $\alpha 4$ , and is well positioned to sterically inhibit DNA binding. It should be noted that the residue numbers in the deposited PDB file are not in register with the residue numbers in this text, which are based on alignment of SlyA orthologs. Comparison with apo-SlyA and SlyA-DNA structures (33) indicates that this salicylate molecule causes the  $\alpha 4$  recognition helix to rotate by  $\sim 35^\circ$  around its axis, disrupting specific contacts with the DNA major groove. Site II is formed by residues from both dimer subunits, almost completely sequestering the salicylate molecule from the solvent. The buried polar groups of salicylate interact with S7' and R14' in  $\alpha 1$  of one subunit and R17 in  $\alpha 1$  and H38 in  $\alpha 2$  from the other subunit. A third salicylate binding site was observed on the surface of each subunit of the dimer. However, this site is adjacent to SlyA residues involved in crystal packing contacts and may not be biologically relevant.

**Mutational analysis of allosteric inhibition of SlyA.** We constructed a series of *slyA* alleles with site-specific mutations of the salicylate-binding pocket in order to test the functional significance of salicylate interactions *in vivo*. When wild-type *slyA* is expressed in *trans* from its native promoter, *pagC* expression increases over 350-fold in inducing medium containing 10  $\mu\text{M}$   $\text{MgCl}_2$  compared to cultures grown with salicylate (Fig. 4A). We tested 8 different mutant alleles for changes in countersilencing activity in response to salicylate. One allele substituting an alanine for tyrosine 66 in site I (T66A) resulted in complete abrogation of salicylate-mediated inhibition, suggesting that T66 is essential for salicylate binding. However, the T66A mutation also decreased *pagC* expression in the absence of salicylate over 25-fold, indicating that it is required for the wild-type activity of SlyA. A second mutant, W34A in site II, also exhibited reduced salicylate-mediated repression. The analysis of these mutants indicates that both site I and site II bind salicylate *in vivo* and that both sites influence SlyA activity. Notably, both T66 and W34 are absolutely conserved in over 55 enterobacterial genera examined in this study (see below), suggesting that these residues are important for SlyA function throughout the *Enterobacteriaceae* (Table S2).

To determine whether salicylate directly inhibits SlyA *in vivo* or stimulates the release of intracellular  $\text{Cu}^{2+}$  from membrane-bound proteins to promote disulfide bond formation, we mutated the single cysteine residue in SlyA, C81. SlyA C81A exhibited a similar salicylate inhibition phenotype as wild-type SlyA, indicating that allosteric inhibition does not occur by disulfide bond formation between cysteine residues *in vivo*. We subsequently generated a chromosomal C81S mutant to determine whether SlyA is directly inhibited by  $\text{Cu}^{2+}$ . Transcription of *pagC* in strains carrying wild-type or C81S *slyA* was reduced approximately 2-fold after the addition of 100  $\mu\text{M}$   $\text{CuCl}_2$  to the growth medium (Fig. 4B). Although this difference was statistically significant ( $P < 0.001$ ), it was also observed in the mutant strain encoding C81S SlyA, indicating that this modest effect is not due to disulfide-dependent tetramerization as proposed for MarR (15). Furthermore, modulation by copper does not appear to be biologically significant in comparison to the 350-fold effect of salicylate.  $\text{Cu}^{2+}$ -mediated derepression of the *marRAB* operon was confirmed under comparable conditions by measuring *marA* expression, which increased approximately 7.5-fold (Fig. 4C).

**Evolutionary analysis of the SlyA TF lineage.** To identify other variables that may have contributed to the evolution of the SlyA lineage, we performed an evolutionary analysis of species representing 60 genera of *Enterobacteriaceae*, including *Candidatus* organisms for which genomic data were available. SlyA is strongly conserved, with orthologs found in 55 organisms, suggesting that SlyA plays a central role in enterobacterial regulatory circuitry. Genera lacking identifiable SlyA orthologs include *Buchnera*, *Hamiltonella*, *Samsonia*, *Thorsellia*, and *Plesiomonas*, which are only distantly related to *Salmonella* and *Escherichia* in comparison to other members of the *Enterobacteriaceae*. Notably, we were also unable to identify an *hns* ortholog in *Plesiomonas*. Phylogenetic analysis reveals five clusters of SlyA orthologs (Fig. 5), with the general

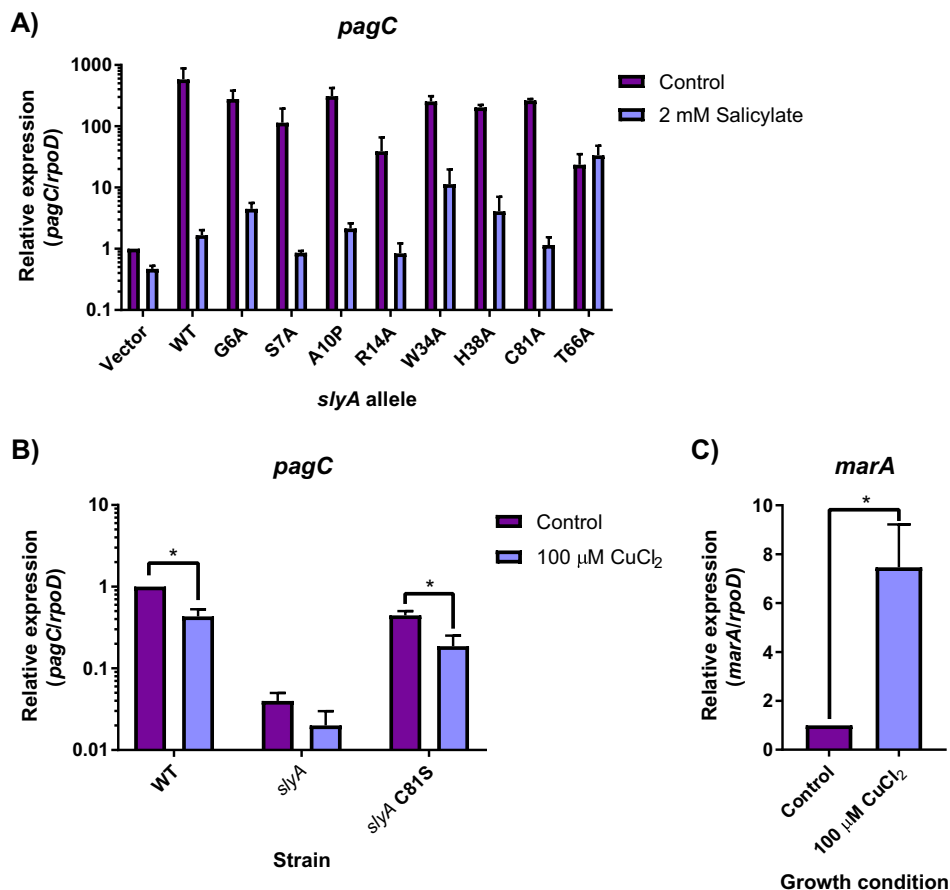


**FIG 4** Genetic analyses of allosteric inhibition of SlyA. Selected residues involved in coordinating SlyA-bound salicylate were mutated in pSL2143, a plasmid expressing *slyA* from its native promoter, and assayed for their ability to restore countersilencing in a chromosomal *slyA* mutant. Cultures were induced in 10  $\mu$ M  $\text{MgCl}_2$ -containing medium in the presence or absence of 2 mM sodium salicylate (A). Levels of *pagC* mRNA were quantified by qRT-PCR and normalized to *rpoD*. The mutant strain carrying the empty pWSK29 vector was included as a control. To determine if SlyA was directly inhibited by  $\text{Cu}^{2+}$  via C81, *pagC* expression was quantified in wild-type or isogenic *slyA* and *slyA* C81S mutant *S. Typhimurium* strains in inducing medium in the presence or absence of 100  $\mu$ M  $\text{CuCl}_2$  (B). To confirm that  $\text{Cu}^{2+}$ -mediated inhibition occurs under these conditions, *marA* transcription was also quantified in the presence or absence of 100  $\mu$ M  $\text{CuCl}_2$  (C). Data represent the mean  $\pm$  SD ( $n = 3$ ). Asterisks indicate  $P < 0.005$ .

structure of the phylogram resembling the genomic tree for *Enterobacteriaceae* (37). SlyA orthologs in enteric pathogens including *E. coli*, *S. Typhimurium*, and *S. flexneri* form cluster I, while cluster II is composed of a more heterogeneous group of organisms, including plant pathogens such as *D. dadantii*, insect endosymbionts like *S. glossinidius*, and more distantly related pathogens such as *Yersinia pseudotuberculosis*. SlyA orthologs in clusters I and II are known to function as pleiotropic regulators, despite significant divergence from the other clusters (28, 31). Clusters III and IV are comprised of environmental organisms such as the plant-associated species *Pantoea agglomerans* and *Phaseolibacter flectens*, while cluster V contains hydrogen-sulfide producing bacteria such as *Pragia fontium*. This degree of conservation suggests that SlyA diverged from the greater MarR family of TFs prior to the divergence of *Enterobacteriaceae* from other bacteria. Although not strongly conserved outside *Enterobacteriaceae*, SlyA orthologs can be detected in selected species throughout the *Gamma-proteobacteria*, indicating that the lineage is ancient. However, the *slyA* gene typically exhibits an AT content (51% in *S. Typhimurium*) marginally higher than that of the chromosomal average (48% in *S. Typhimurium*), suggesting that it may have been duplicated through an ancient transfer event.

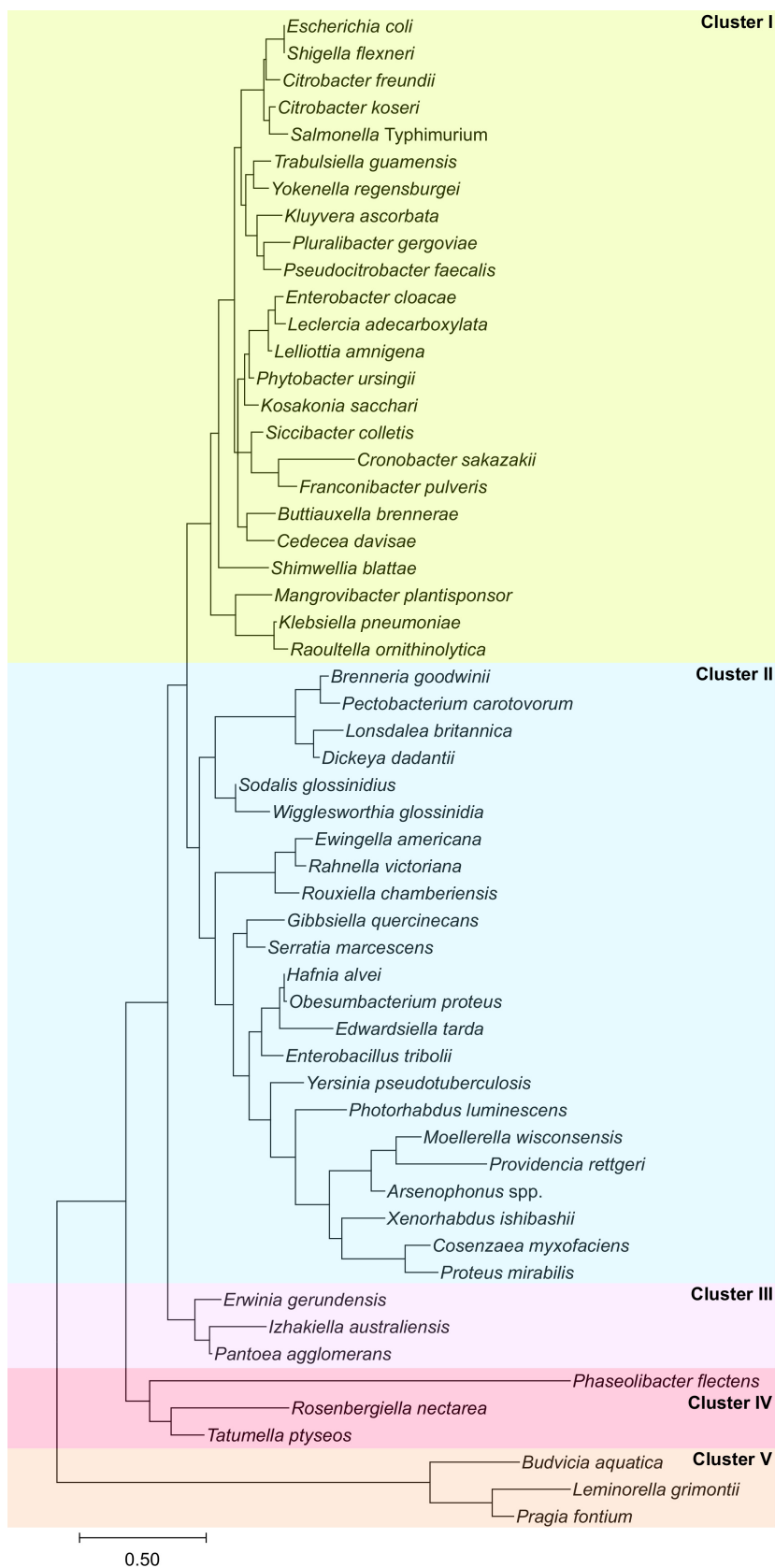


**FIG 5** The SlyA TF lineage in *Enterobacteriaceae*. The evolutionary history of the SlyA TF lineage was inferred using the maximum likelihood method and the Le-Gascuel model (89) with Mega X software (90). The tree is drawn to scale with the branch length representing the number of substitutions per site.

(Continued on next page)

To determine if allosteric inhibition is likely to be conserved throughout the SlyA lineage, we aligned the sequences of SlyA orthologs from different bacterial species to analyze the conservation of residues involved in salicylate binding (Table S2). Cluster I exhibited nearly complete conservation of the salicylate-binding residues, with only four of 24 genomes encoding polymorphisms. Cluster II exhibited the greatest variation, with 16 of 23 genomes encoding polymorphisms, including 10 which encoded the polymorphism H38Y. We identified only one polymorphism in site I in six genomes, a T32I substitution, suggesting that site I is particularly important for SlyA function. As further evidence of the importance of site I, a T66A mutation abrogated allosteric inhibition of SlyA. The central residues of site II (R14, W16, R17, and W34) are similarly conserved, suggesting that these residues are also important for SlyA function. We were able to mutate two of these residues (Fig. 4A), R14 and W34, and found that W34 is also involved in allosteric inhibition. Individual polymorphisms such as T32I and H38Y appear to have evolved independently in multiple clusters, suggesting purifying selection, although their effect on SlyA activity is currently unknown. Alignment of SlyA protein sequences from representative species of each of the five clusters revealed that most sequence variation occurs in the carboxyl terminus oligomerization domain (Fig. S2), suggesting that ligand sensitivity and DNA binding are conserved features of the SlyA lineage.

As the ancestral function of MarR TFs is the negative regulation of genes encoding drug efflux pumps, a function that is conserved in *S. Typhimurium*, we examined *slyA* orthologs throughout the *Enterobacteriaceae* for linkage to flanking genes of known or hypothetical function: *slyB*, which encodes a putative outer membrane lipoprotein with no observed phenotype; *ydjJ*, which encodes a hemolysin D homolog; and *ydjK*, encoding the efflux pump (Fig. 6A and B). It should be noted that *ydjJ* also exhibits homology to *emrA*, which encodes an antimicrobial efflux pump-associated protein linked to and regulated by another MarR family TF called MprA or EmrR (38, 39). We found that cluster I exhibited the strongest linkage, with 100%, 95%, and 100% linkage to *ydjJ*, *ydjK*, and *slyB*, respectively, while cluster V, containing the hydrogen sulfide-producing bacteria, exhibited no linkage to *slyA* for any of the genes examined. Outside cluster V, *slyB* was strongly associated with *slyA*, exhibiting 76% linkage overall. However, the *ydj* operon was not strongly linked outside cluster I, exhibiting 26%, 33%, and 33% linkage in clusters II, III, and IV, respectively. In contrast, although *marR* was absent from 26 of the enterobacterial species examined, *marR* was linked to *marAB* in every *marR*-carrying species. This suggests that the primary function of MarR is to regulate the *marRAB* operon, and MarR consequently does not play an important role in enterobacterial regulatory circuitry. In contrast, the loss of the ancestral linkage between *slyA* and *ydjJ* outside cluster I suggests that the SlyA lineage has evolved to serve a distinct function.

The *ydjJK* operon does not appear to have been exchanged for another drug efflux system (Fig. 6C). Sequences homologous to the proximal portion of the *ydjI* gene are detectable even in species that have not retained functional coding sequences (e.g., *Y. pseudotuberculosis*). However, a 100-bp segment of the *ydjI-slyA* intergenic region, beginning approximately 95 bp upstream of the *slyA* start codon, has undergone extensive mutation (Fig. 6C), suggesting in *cis* evolutionary adaptation in the *slyA* lineage of TFs. We examined the regions upstream of *slyA* in several related species of three genera, *Escherichia*, *Salmonella*, and *Yersinia*, to better understand the recent evolution of this region, and observed that the *ydjI-slyA* intergenic regions exhibit

#### FIG 5 Legend (Continued)

The *slyA* genes have evolved in five major phylogenetic clusters: cluster I comprises most enteric species, including *S. Typhimurium* and *E. coli*; cluster II is heterogeneous, containing more distantly related pathogenic species from *Proteus* and *Yersinia*, as well as endosymbionts like *Sodalis*; clusters III and IV contain several plant-associated bacteria, such as *Pantoea agglomerans* and *Phaseolibacter flectens*; cluster V is comprised of hydrogen sulfide-producing bacteria. (A multiple sequence alignment of selected SlyA orthologs can be found in Fig. S2.)

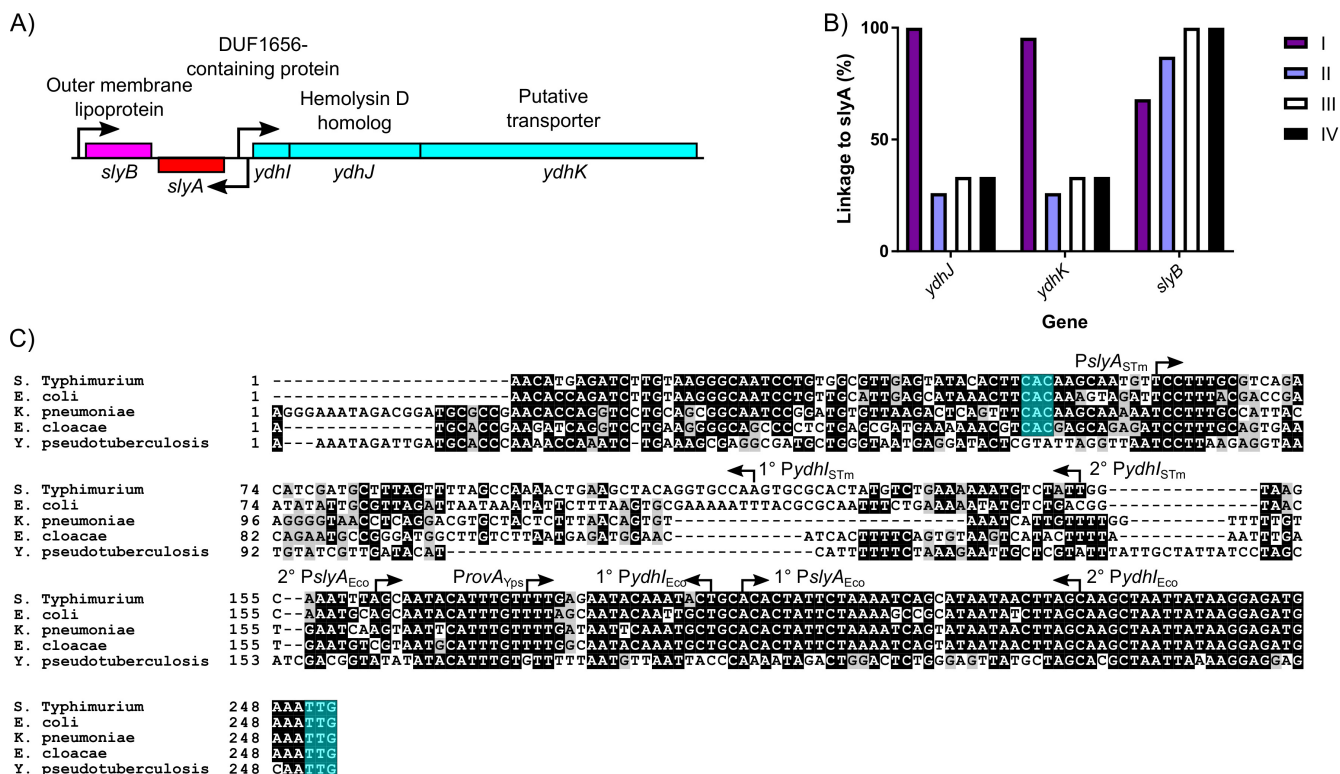


**FIG 6** Genetic linkage and *cis*-regulatory evolution of *slyA* in *Enterobacteriaceae*. The *slyA* region of *S. Typhimurium* and closely related enteric species is diagrammed in panel A. Arrows indicate TSSs, and boxes represent protein coding sequences. The *ydhIJK* efflux pump operon is transcribed divergently from *slyA*. A protein of unknown function is encoded by *ydhI*, and *ydhJ* and *ydhK* encode a hemolysin D/EmrA homolog and a transporter protein, respectively. *slyB* encodes a putative outer membrane lipoprotein, transcribed convergently to *slyA*. The linkage of *slyA* to *slyB*, *ydhJ*, and *ydhK* is determined for all of the species from clusters I to IV shown in Fig. 5 (B). Species from cluster V do not exhibit linkage to these genes and are not shown. A multiple sequence alignment of the *slyA* promoter region from the closely related species *S. Typhimurium*, *E. coli*, *K. pneumoniae*, and *E. cloacae*, as well as more distantly related *Y. pseudotuberculosis* (C). Arrows indicate the position and orientation of previously characterized TSSs (30, 55, 57). Where multiple TSSs have been identified, the primary (1°) and secondary (2°) start sites are indicated. The *slyA* (positions 248 to 250) and *ydhI* (positions 47 to 70, dependent on the species) start codons are highlighted in teal when present. (Alignments of this region from representative species of *Salmonella*, *Escherichia*, and *Yersinia* are shown in Fig. S3. A phylogenetic analysis of the *slyA* promoter region of a subset of genera is shown in Fig. S4.)

considerable divergence between genera and conservation within genera (Fig. S3). A comparison between the *ydhI-slyA* intergenic regions of *Escherichia coli* and *Salmonella Typhimurium* and those of *Klebsiella pneumoniae* and *Enterobacter cloacae* revealed similar degrees of divergence between each genus, suggesting that an ancestral allele can no longer be defined. A phylogenetic analysis of *slyA* upstream regions in a representative subset of the species described above demonstrated extensive variation throughout the *Enterobacteriaceae* (Fig. S4). However, this variation did not always correlate with SlyA coding region clusters. Although the intergenic regions of cluster I are closely related and may have coevolved with their respective coding sequences, the other clusters are more variable, and some intergenic regions may have evolved independently of their coding sequences.

Examination of the *ydhI-rovA* region in *Yersinia* spp. reveals that *rovA* in *Y. pseudotuberculosis* (Fig. 6C) and *Yersinia pestis* (Fig. S3) is not linked to a functional *ydhIJK* operon, whereas *ydhIJK* is retained in *Yersinia enterocolitica*. This indicates that *ydhIJK* was not lost by the former species until after the divergence of *Yersinia* from other *Enterobacteriaceae* and suggests that other species of *Enterobacteriaceae* are also likely to have lost *ydhIJK* recently, as each became adapted to its own specific niche. This represents an example of parallel evolution, with multiple species independently losing *ydhIJK* to accommodate *in cis* evolution as their respective SlyA orthologs adapted to new roles.

**Functional characterization of a distantly related SlyA ortholog.** To understand how the SlyA lineage adapted to its emergent role as an important pleiotropic

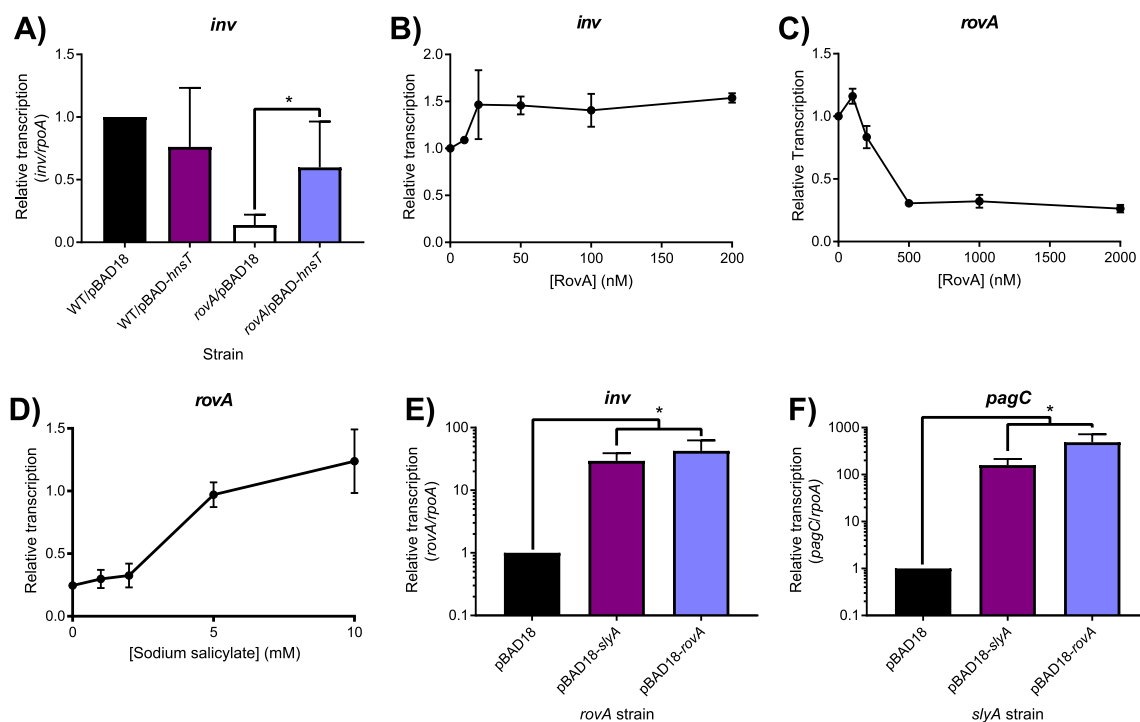


**FIG 7** Environmentally responsive repressing and countersilencing functions are conserved in the SlyA TF lineage. To determine whether RovA functions as a countersilencer in *Y. pseudotuberculosis*, transcription of the Rov-regulated *inv* gene was quantified by qRT-PCR in wild-type or *rovA* mutant strains expressing *hnsT<sub>EPEC</sub>* which inhibits H-NS (A). Although *inv* expression is decreased in a *rovA* mutant strain, expression is fully restored by the inhibition of H-NS, indicating that RovA functions as a countersilencer. IVT assays of the *inv* regulatory region in the presence of increasing RovA concentrations detected only a minimal impact on transcription levels, suggesting that RovA is unlikely to function as a classical activator (B). IVT assays of *rovA* in the presence of increasing RovA concentrations demonstrate that RovA functions as an autorepressor (C). RovA remains sensitive to inhibition by small aromatic carboxylate molecules, as increasing concentrations of sodium salicylate inhibited RovA-mediated *rovA* repression in IVT assays (D). All IVT data represent the mean  $\pm$  SEM ( $n \geq 3$ ). Reciprocal complementation studies were performed by providing either *rovA* or *slyA* in *trans* expressed from the arabinose-inducible pBAD18 vector in *rovA* or *slyA* mutant *Y. pseudotuberculosis* and *S. Typhimurium* strains, respectively, and measuring transcription of *inv* (E) and *pagC* (F) via qRT-PCR. Transcript levels are normalized to *rpoA* in both species, and data represent the mean  $\pm$  SD ( $n = 3$ ). Asterisks indicate  $P < 0.05$ .

regulatory protein in the *Enterobacteriaceae*, we compared the functions of SlyA from *S. Typhimurium* (SlyA<sub>STM</sub>) and RovA of *Y. pseudotuberculosis* and *Y. enterocolitica*, a relatively divergent ortholog that also functions as a countersilencer (28–30, 40). RovA of *Y. pseudotuberculosis* exhibits 76% identity with SlyA<sub>STM</sub> (Fig. S2). RovA is essential for virulence in *Y. enterocolitica* and *Y. pestis* (28, 41) and has been suggested to function both as an activator, interacting with RNAP (42), and as a countersilencer, alleviating H-NS-mediated repression (29, 30, 40). Notably, direct activation has not been demonstrated for any other member of the SlyA lineage, and the most direct evidence to suggest that RovA functions as an activator is derived from IVT studies using small linear fragments of DNA as a template (42). We have previously shown that small linear fragments are not necessarily representative of physiological regulatory events in intact cells and can generate spurious results in IVT assays (17). Genetic analysis of the *inv* gene, which is positively regulated by RovA, in an *hns* mutant strain of *E. coli* also suggested that RovA functions as both a countersilencer and an activator. However, these experiments failed to consider the potential contribution of the H-NS paralog StpA, which is upregulated in *hns* mutants and can provide partial complementation (43, 44), which complicates the interpretation of regulatory studies in an *hns* mutant strain.

We attempted to corroborate the published findings by performing IVT analysis of *inv* expression in the presence of RovA. However, expression of *inv* exhibited only a very modest (~1.5-fold) increase following the addition of RovA (Fig. 7A), which became saturated at a 20 nM concentration; these results are not supportive of direct *inv*

activation by RovA. In contrast, RovA was confirmed to function as an autorepressor, like other MarR family TFs, as IVT analysis demonstrated a 4-fold decrease in *rovA* expression following the addition of RovA protein, with the effect reaching saturation at a 500 nM concentration (Fig. 7B). RovA has also retained the ability to respond to salicylate (Fig. 7C), despite the presence of an H38Y substitution in the second salicylate-binding pocket (Table S2), as 5 mM salicylate completely inhibited RovA-mediated repression, similar to our observations with SlyA. It is also notable that RovA has retained salicylate sensitivity despite the loss of the linked YdhIJK efflux pump in *Y. pseudotuberculosis*. To prove that RovA functions as a countersilencer in *Y. pseudotuberculosis*, we measured *inv* expression in wild-type and *rovA* mutant strains expressing H-NST from enteropathogenic *E. coli* (H-NST<sub>EPEC</sub>). Mutations in *hns* cannot be generated in *Yersinia*, as *Yersinia* spp. carry a single essential *hns* gene, unlike many other members of the *Enterobacteriaceae*, which carry *hns*-like genes such as *stpA* that are able to partially compensate for the loss of *hns*. H-NST<sub>EPEC</sub> is a truncated *hns* homolog that has been demonstrated to function as a dominant negative form of H-NS by binding and inhibiting the activity of wild-type H-NS protein (45). The expression of *inv* in *rovA* mutant bacteria was approximately 4-fold lower than in wild-type cells (Fig. 7D). However, *inv* expression was fully restored upon inhibition of H-NS by *hnsT*<sub>EPEC</sub>, demonstrating that RovA functions solely as a countersilencer of the *inv* gene. The *rovA* and *slyA* genes are capable of complementing each other in both *S. Typhimurium* and *Y. pseudotuberculosis* when expressed in *trans* (Fig. 7E and F), upregulating both *inv* and *pagC*, further indicating that RovA functions as a countersilencer, like SlyA. Together, these observations demonstrate that RovA has retained the ancestral characteristic of environmentally-responsive repression exhibited by other members of the MarR TF family, despite being one of the most divergent members of the SlyA lineage. However, in contrast to MarR TFs outside the SlyA lineage, it is also able to function as a countersilencer of horizontally-acquired genes, as exemplified by *inv*.

**SlyA countersilencing requires high expression levels.** It is interesting that SlyA does not play a major regulatory role in *Escherichia coli*, the best-studied member of the *Enterobacteriaceae*. SlyA is known to regulate only two *E. coli* genes, *hlyE* and *fimB* (46–48), despite exhibiting a high degree of homology (91% identity) to SlyA in *S. Typhimurium*. To better understand the different roles of SlyA in the regulatory hierarchy of *E. coli* and *S. Typhimurium*, we performed a comparative genetic analysis of the *S. Typhimurium* (*slyA*<sub>STM</sub>) and *E. coli* (*slyA*<sub>Eco</sub>) alleles. In allelic exchange experiments, the *slyA*<sub>STM</sub> coding sequence was swapped with *slyA*<sub>Eco</sub> to determine the effect on the expression of the countersilenced *S. Typhimurium* *pagC* gene (Fig. 8A). We observed that SlyA<sub>Eco</sub> is able to countersilence the expression of *pagC* similarly to SlyA<sub>STM</sub>, suggesting that the diminished role of SlyA in *E. coli* is not attributable to differences in protein sequence. This suggested that the importance of different SlyA lineage proteins within their respective regulatory networks may be the result of the different *in cis* evolutionary pathways identified in our phylogenetic analysis (Fig. 6 and Fig. S4), resulting in differences in levels of expression. To test this hypothesis, *slyA* intergenic region-ORF chimeras were constructed and assessed for their ability to countersilence *pagC*. To avoid potentially confounding results due to multiple transcriptional start sites (TSSs), we exchanged the intergenic regions beginning immediately upstream of each start codon. Countersilencing was assessed in a *slyA* mutant carrying pKM05, a plasmid with the *slyA*<sub>STM</sub> ORF transcribed by the *E. coli* promoter (P*slyA*<sub>Eco</sub>), or pKM07, a plasmid with the *slyA*<sub>STM</sub> ORF transcribed by its native promoter (P*slyA*<sub>STM</sub>). Although *pagC* expression was similar with either construct under noninducing conditions, expression was approximately 10-fold lower with *slyA* expressed from P*slyA*<sub>Eco</sub> under inducing conditions (Fig. 8B), suggesting that the diminished role of SlyA in *E. coli* is at least partially attributable to differences in *slyA* expression levels in *S. Typhimurium* and *E. coli*. Although *slyA* expression driven by P*slyA*<sub>Eco</sub> is only slightly lower under noninducing conditions, it is approximately 3-fold greater when driven by P*slyA*<sub>STM</sub> under inducing conditions (Fig. 8C), suggesting that P*slyA*<sub>Eco</sub> is less

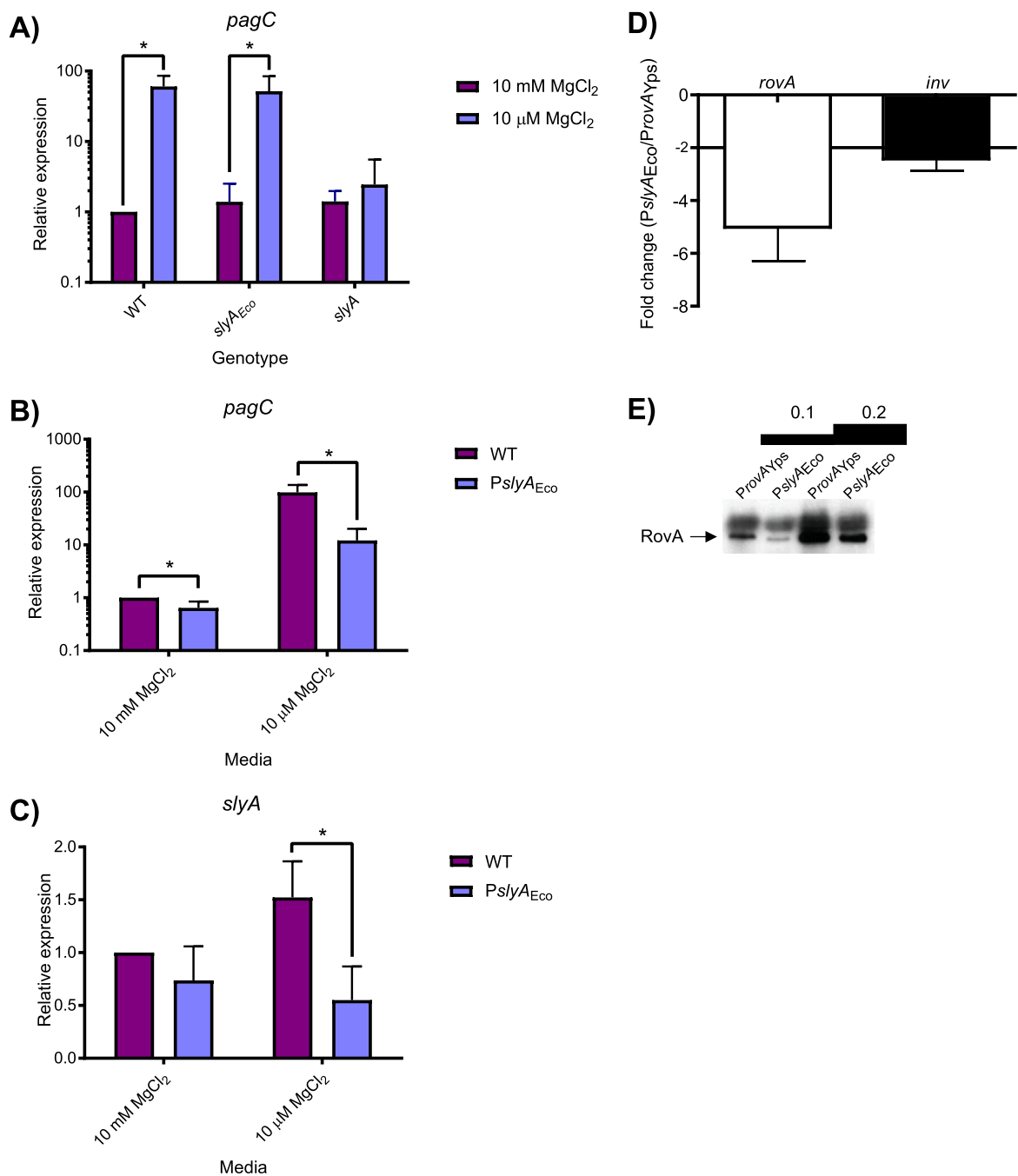


**FIG 8** *S. Typhimurium* SlyA is a more effective countersilencer than *E. coli* SlyA due to higher expression levels. Expression of the SlyA countersilenced *pagC* gene was measured by qRT-PCR in *S. Typhimurium* strains carrying wild-type *slyA*, *slyA<sub>Eco</sub>*, or mutant *slyA* under either inducing (10 μM MgCl<sub>2</sub>) or noninducing (10 mM MgCl<sub>2</sub>) conditions (A). Expression of *pagC* (B) and *slyA* (C) was compared in *S. Typhimurium* strains in which *slyA* transcription was driven by either the wild-type (WT) or *E. coli* (*PslyA<sub>Eco</sub>*) *slyA* promoter. Transcript levels are normalized to *rpoD*, and data represent the mean ± SD (*n* = 3). Asterisks indicate *P* ≤ 0.05. To compare the strength of the native *rovA* promoter (*Prova<sub>Yps</sub>*) and *PslyA<sub>Eco</sub>*, the native *rovA* promoter was replaced with the corresponding sequence from *E. coli*, and the resulting chimera was examined for its ability to regulate the *RovA* targets *rovA* and *inv* in *Y. pseudotuberculosis*. Transcripts were quantified by qRT-PCR and normalized to *gyrB* (D). *RovA* protein levels were confirmed by immunoblot analysis using 0.1 and 0.2 OD<sub>600</sub> of culture after 6 h of growth (left two and right two lanes, respectively) (E). The position of *RovA* is indicated by an arrow.

responsive to environmental signals associated with virulence gene expression in *Salmonella* and thus is unable to regulate *slyA* expression in a manner appropriate for countersilencing. Parallel experiments in *Y. pseudotuberculosis* revealed that *rovA* is also more strongly expressed from its native promoter (*Prova<sub>Yps</sub>*) than from a chimera

expressing *rovA* from *PslyA<sub>Eco</sub>* (Fig. 8D and E), despite the fact that *ProvA<sub>Yps</sub>* has diverged much more significantly from both *PslyA<sub>Eco</sub>* and *PslyA<sub>STm</sub>* than *PslyA<sub>Eco</sub>* and *PslyA<sub>STm</sub>* have diverged from each other (Fig. S4).

## DISCUSSION

The ancient MarR family of transcription factors is represented throughout the bacterial kingdom and in many archaeal species (36). This study examines how the SlyA/RovA lineage of MarR TFs in the *Enterobacteriaceae* has evolved to acquire the novel function of countersilencing. Our observations demonstrate that SlyA proteins have retained some ancestral features, including the environmentally-responsive repression of small molecule efflux systems, while acquiring the ability to act as pleiotropic countersilencers of horizontally-acquired genes. The latter role has been facilitated by the parallel evolution of *cis*-regulatory elements that support higher levels of gene expression.

SlyA, like other MarR family TFs, is subject to allosteric inhibition by small aromatic carboxylate compounds such as salicylate, which bind and stabilize the SlyA dimer in a conformation unfavorable for DNA binding (Fig. 2; also see Fig. S1 in the supplemental material). However, the specific structure and arrangement of the effector binding sites vary significantly among the MarR family. Our structural data indicate that SlyA binds a total of six salicylate molecules per dimer, at least four of which are likely to be biologically relevant (Fig. 3). Although the general structure and architecture of the salicylate-SlyA complex are similar to complexes formed by other MarR TFs, including MarR (8) and MTH313 from *Methanobacterium thermoautotrophicum* (49), the various TFs differ significantly in their specific interactions with salicylate. MarR binds a total of four salicylate molecules per dimer, whereas MTH313 binds only two (Fig. 3D and E). All four salicylate-binding sites in MarR flank the wHTH domain and are partially exposed to solvent, whereas none of these sites corresponds to the salicylate binding sites of SlyA, potentially accounting for the significant differences in affinity for aromatic carboxylates between the two proteins. MTH313 binds salicylate asymmetrically at sites similar to sites I and II of SlyA, binding only one salicylate molecule per monomer. It is possible that the structural variability in the MarR family with respect to salicylate binding reflects an inherent evolutionary flexibility and ligand promiscuity. The MarR family sensor region may have evolved to interact with a variety of small molecules, and salicylate may simply represent a promiscuous probe for potential interactions. Recent studies have suggested that the true ligand of MarR may be copper, liberated from membrane-associated proteins during oxidative stress induced by xenobiotic agents. Copper reportedly oxidizes a cysteine residue (C80) to promote disulfide bond formation between MarR dimers, resulting in tetramerization and inhibition of DNA binding (15). As almost all characterized MarR TFs have a reactive cysteine residue corresponding to a region near site II of SlyA, we considered that cysteine oxidation, which has also been described in the MarR family TF OhrR (50), might occur in the SlyA lineage as well. However, mutation of C81, the lone cysteine residue in *SlyA<sub>STm</sub>*, had a negligible effect on SlyA activity in either the presence or absence of salicylate. The addition of copper to the growth medium had a minimal impact on SlyA activity and was unaffected by mutation of C81, indicating that cysteine oxidation is not a general mechanism for the allosteric inhibition of MarR family TFs. Furthermore, the high affinity of SlyA for aromatic carboxylates (Fig. S1) and the conservation of binding pocket residues (Table S2) reported in this study suggest that environmental sensitivity and allosteric inhibition are conserved features of SlyA activity in its new regulatory role.

A phylogenetic analysis of SlyA orthologs in the *Enterobacteriaceae* demonstrates that the SlyA lineage is strongly conserved, even in endosymbiotic species exhibiting significant genome loss (Fig. 5 and Fig. S2). This suggests that SlyA has a central and essential role in the transcriptional regulatory networks of these species. For example, a recent analysis of the endosymbiont *Wigglesworthia glossinidia* found that *slyA* is subject to significant evolutionary constraints (51). This conservation does not appear to be due to its role as a regulator of antimicrobial resistance, as *slyA* does not exhibit

significant linkage to the efflux pump operon *yhjJK*, outside the enteric pathogens in cluster I (Fig. 6). Rather, SlyA proteins appear to function predominantly as pleiotropic countersilencers, facilitating the integration of horizontally-acquired genes, including virulence genes, into existing regulatory networks. A general countersilencing role has been suggested in multiple enterobacterial species including *E. coli* (19, 48), *Salmonella* (17, 20, 21), and *Shigella* (32) in cluster I and *Yersinia* (31, 52) and *Serratia* and *Pectobacterium* (*Erwinia*) (25) in cluster II. Although similar evidence does not currently exist for the endosymbionts of cluster II, this may simply reflect the limited genetic analyses that have been performed in these species thus far.

To understand the evolutionary adaptations to accommodate countersilencing by the SlyA/RovA lineage, we compared three orthologs, *slyA*<sub>STM</sub>, *slyA*<sub>Eco</sub>, and *rovA*. The *slyA*<sub>STM</sub> and *rovA* genes are essential for *Salmonella* and *Yersinia* virulence, whereas *slyA*<sub>Eco</sub> plays a negligible role in *E. coli*, despite exhibiting far greater similarity to *slyA*<sub>STM</sub> than *rovA*. These differing roles are attributable to differences in expression, as SlyA<sub>Eco</sub> is able to function as a countersilencer in *S. Typhimurium* when its expression is driven by the *S. Typhimurium* promoter (Fig. 6). We also observed that *slyA*<sub>Eco</sub> transcription is significantly reduced in medium with low Mg<sup>2+</sup> concentrations, a condition associated with the *Salmonella*-containing vacuole (SCV) of macrophages, in which SlyA cooperates with the response regulator PhoP to countersilence virulence genes necessary for intracellular survival (17). This suggests that the diminished role of *slyA*<sub>Eco</sub> in *E. coli* may result from its inability to respond to appropriate environmental cues. This is further reinforced by the observation that RovA of *Yersinia* spp. is able to function as a countersilencer in *S. Typhimurium* when expressed in *trans* from an inducible promoter and that the *rovA* promoter of *Y. pseudotuberculosis* drives *rovA* transcription more strongly than *PslyA*<sub>Eco</sub> in a chimeric strain (Fig. 8). This suggests that evolution of the SlyA-RovA lineage in *trans*, particularly DNA binding specificity, has played only a minor role since the divergence of the *Enterobacteriaceae*. This is further supported by a comparison of distantly-related SlyA orthologs, which exhibit most sequence divergence in the C-terminal oligomerization domain and not the N-terminal region containing the wHTH (Fig. S2). We conclude that the ability of a given SlyA ortholog to serve as a countersilencer is contingent on its level and pattern of expression, which may be the product of both transcriptional and posttranscriptional activity, as mutations altering TSS location will also alter the 5' untranslated region of the *slyA* transcript. Notably, another group recently demonstrated a significant expansion of the SlyA regulon in *E. coli* when *slyA*<sub>Eco</sub> is overexpressed, with 30 operons exhibiting regulation by SlyA, 24 of which are also repressed by H-NS (34), indicating that SlyA<sub>Eco</sub> is theoretically capable of functioning as a countersilencer but is not expressed appropriately. In *S. Typhimurium*, the appropriate conditions are those associated with the SCV. However, SlyA orthologs in other species such as the plant pathogens and endosymbionts of cluster II are likely to require expression under different conditions corresponding to their respective environmental niches. The loss of the divergently-transcribed *yhjJK* operon in *Y. pseudotuberculosis* and other enteric species may be a consequence of genetic alterations to enhance *rovA* expression as well as the redundancy of drug efflux pumps. An additional possibility is that enhanced *slyA/rovA* expression might result in hyperrepression of *yhjJK*, which would negate the usefulness of the pump to the cell. Even the plant pathogens such as *D. dadantii* and *P. carotovorum*, which are most likely to encounter small phenolic compounds in the plant environment (53), have failed to retain *yhjJK*. It is also notable that the *slyA* orthologs in the four species (*E. coli*, *S. Typhimurium*, *Y. enterocolitica*, and *Y. pseudotuberculosis*) in which the transcriptional start sites have been characterized initiate transcription at different positions (30, 54–57), indicating that each species has evolved its *cis*-regulatory circuit independently (Fig. 6).

Previous studies have demonstrated that regulatory evolution can promote adaptation to new niches (58). The SlyA/RovA TF lineage provides a unique example of parallel regulatory evolution to achieve a common functional objective. Throughout the *Enterobacteriaceae*, the associated *yhjJK* pump genes have been repeatedly lost,

yet their regulators have been retained, presumably to facilitate the evolution of an appropriately responsive regulatory circuit to enable countersilencing. This suggests that SlyA/RovA proteins possess intrinsic features that predispose them for a countersilencing role, perhaps the abilities to respond to environmental stimuli and to recognize a variety of AT-rich target DNA sequences. Studies are under way to characterize these features and to determine their contribution to the evolutionary capacity of *Enterobacteriaceae*.

## MATERIALS AND METHODS

**Bacterial strains and general reagents.** All oligonucleotides and plasmids used in this study are described in Table S3 in the supplemental material. Unless otherwise indicated, bacteria were grown in Luria-Bertani (LB) broth with agitation. *Salmonella enterica* serovar Typhimurium strains were constructed in the ATCC 14028s background and grown at 37°C, unless otherwise indicated. The 14028s *slyA* mutant strain was described previously (17). *Yersinia pseudotuberculosis* YPIII (59) and YP107 (60) (a gift from P. Dersch, Helmholtz Centre for Infection Research) were used as the wild-type and *rovA* strains, respectively, and grown at 24°C. A *ydhIJK* deletion mutant was constructed using the  $\lambda$ -Red recombinase system (61) and oligonucleotides WNP318 and WNP319. A *slyA ydhIJK* strain was generated by introducing the *slyA::Cm* cassette from 14028s *slyA::Cm* (17) to 14028s *ydhIJK* via P22HTint-mediated transduction. To exchange the wild-type *S. Typhimurium slyA* coding sequence with the *E. coli* allele, *S. Typhimurium slyA* was replaced with a *thyA* cassette, via FRUIT (62), using the oligonucleotides STM-*slyA*-targ-F and STM-*slyA*-targ-R. The *slyA* coding sequence from *E. coli* K-12 was then amplified using the primers STM-Eco-*slyA*-F and STM-Eco-*slyA*-R, which include 40 and 41 bases, respectively, from the regions flanking the *S. Typhimurium slyA* coding sequence. This fragment was electroporated into the *slyA::thyA* mutant strain, and the resulting transformants were plated on minimal medium containing trimethoprim, as described for the FRUIT method (62), to select for replacement with the *E. coli slyA* allele.

The chromosomal C81S *slyA* mutation (TGC→AGC) was generated by cloning a 1-kb fragment encoding the C81S mutation into the suicide vector pRDH10 (63) using Gibson Assembly (New England Biolabs, Ipswich MA). The Gibson assembly reaction included PCR products generated with primers JKP736/JKP737 and JKP738/JKP739 and genomic *S. Typhimurium* DNA as well as BamHI-digested pRDH10 to generate pJK723. For integration of *slyA* C81S into the chromosome, S17-1 $\Delta$ pir (64)/pJK723 was mated with *S. Typhimurium* 14028s/pSW172 (65), plated onto LB + 20  $\mu$ g ml<sup>-1</sup> chloramphenicol, and incubated at 30°C overnight. Chloramphenicol- and carbenicillin-resistant (Cm<sup>r</sup> Carb<sup>r</sup>) colonies that were isolated represented a single-crossover event of pJK723 (Cm<sup>r</sup>) plasmid into the *slyA* region of *S. Typhimurium* 14028s (Carb<sup>r</sup>). Selection for the second crossover event to replace wild-type *slyA* with a *slyA* C81S mutation was performed by plating 0.1 ml of an overnight culture of the Cm<sup>r</sup> Carb<sup>r</sup> colony onto LB + 5% sucrose plates and incubating at 30°C overnight. Colonies were then streaked onto LB plates at 37°C, and putative 14028s *slyA* C81S colonies were confirmed by DNA sequencing.

To perform allelic exchange analysis of the *rovA* and *slyA*<sub>Eco</sub> promoters, YPTB007 was generated from *Y. pseudotuberculosis* IP32953 (66). YPTB007 is a derivative of IP32953 in which the native *rovA* promoter was replaced with the *E. coli slyA* promoter. Briefly, the 691 bp 5' of the native *rovA* gene were replaced with the 292 bp 5' of the *E. coli slyA* gene using pSR47s (67) and homologous recombination. Replacement was confirmed by PCR amplification of the intergenic region and DNA sequencing.

**Cloning.** pSL2143 was generated by amplifying the *slyA*<sub>STM</sub> region, including its native promoter, with primers *slyA*Comp-F and *slyA*Comp-R and ligating into pWSK29 (68) digested with EcoRV. The G6A, S7A, A10P, R14A, W34A, H38A, T66A, and C81A mutants were generated with their respective mutagenic primer pairs (Table S3) using the QuikChange XL site-directed mutagenesis kit (Agilent Technologies, Santa Clara, CA) according to the manufacturer's protocol. A 2,249-bp region containing both *slyA* and *ydhI* was amplified by PCR using the primers SlyAreg-F and SlyAreg-R. The resulting fragment was digested with BamHI and HindIII and ligated into the low-copy-number IVT scaffold vector pRW20 (17) to generate pRW39. An IVT target containing the 2,379-bp *rovA* region from *Y. pseudotuberculosis* was generated using the primers BamHI-*rovA*-F and EcoRI-*rovA*-R. The resulting fragment and pRW20 were both digested with BamHI and EcoRI and ligated together to construct pRW54. An IVT target containing the 2,708-bp *inv* region from *Y. pseudotuberculosis* was generated via PCR using the primers BamHI-*inv*-F and EcoRI-*inv*-R. The resulting fragment and pRW20 were both digested with BamHI and EcoRI and ligated together to construct pRW55. To perform *rovA* and *slyA* complementation studies, both genes were cloned into the arabinose-inducible expression vector pBAD18 (69). The *rovA* gene was amplified using the oligonucleotides EcoRI-*rovA*-F and KpnI-*rovA*-R. The *slyA* gene was amplified using the oligonucleotides EcoRI-*slyA*-F and KpnI-*slyA*-R. Both fragments were digested with EcoRI and KpnI and ligated into pBAD18, generating pRW58 (*slyA*) and pRW59 (*rovA*). pRW60 was constructed by cloning an N-terminal 6 $\times$ His-tagged copy of *rovA* into pTRC99a (70). The *rovA* gene was amplified from YPIII genomic DNA by PCR using the oligonucleotides 6HisRovA-F and 6HisRovA-R. The resulting fragment and pTRC99a were digested with NcoI and BamHI and ligated together. An *E. coli* P<sub>*slyA*</sub>-5. *S. Typhimurium slyA* coding sequence chimera was constructed using overlapping PCR. The *slyA-ydhIJK* intergenic region was amplified from *E. coli* K-12 genomic DNA using primers KMP178 and KMP206 and from *S. Typhimurium* 14028s using oligonucleotides KMP177 and KMP206. The corresponding *slyA* ORF from *S. Typhimurium* was amplified with primers KMP207 and KMP181. The ORF and promoter segments were amplified along with 40 bp of complementary overlapping sequence. Products from the ORF and promoter reactions were mixed 1:1 and amplified using primers KMP178 (*E. coli*) or KMP177 (*S.*

Typhimurium) and Kmp181 to amplify the promoter/ORF chimeras. The resulting fragment and pTH19Kr (71) were digested with BamHI and HindIII and ligated together, generating pKM05 (*E. coli* promoter) and pKM07 (*S. Typhimurium* promoter). Plasmids were transformed into *S. Typhimurium* 14028s *slyA* for gene expression analysis. The *hnsT* coding sequence was amplified from E2348/69 genomic DNA using the oligonucleotides EcoRI-hnsT-F and HindIII-hnsT-R. Both pBAD18 and the resulting PCR fragment were digested with EcoRI and HindIII, agarose gel-purified, and ligated together to generate pRW57.

**Fusaric acid resistance assays.** Cultures were grown overnight in LB broth at 37°C and then diluted 1:100. Thirty microliters of this dilution was added to 270  $\mu$ l of LB containing 30  $\mu$ g/ml freshly-prepared fusaric acid in 100-well BioScreen plates (Growth Curves, Piscataway, NJ). Cultures were grown with continuous maximum shaking at 37°C, and regular OD<sub>600</sub> measurements were taken on a BioScreen C MBR. Fresh 20-mg/ml stock solutions of fusaric acid were prepared in dimethyl formamide (DMF).

**In vitro transcription.** IVT assays were performed essentially as previously described (17) with the following modifications. All SlyA IVT assays were performed at 37°C. All RovA IVT assays were performed at 24°C. Where indicated, sodium salicylate was added to IVT reaction mixtures prior to the addition of SlyA or RovA. All oligonucleotides and templates used in IVT reactions are indicated in Table S4.

**RNA isolation and qRT-PCR.** RNA was purified using TRIzol (Life Technologies, Carlsbad, CA) according to the manufacturer's protocols. cDNA was generated using the QuantiTect reverse transcription kit (Qiagen, Hilden, Germany) and quantified in a Bio-Rad CFX96 (Bio-Rad, Hercules, CA), using SYBR Green master mix (72).

For the analysis of *pagC* expression under inducing conditions, *S. Typhimurium* cultures were grown to early stationary phase (OD<sub>600</sub>  $\approx$  2.0) at 37°C in LB broth and then washed three times in N-minimal medium containing either 10  $\mu$ M (inducing) or 10 mM (noninducing) MgCl<sub>2</sub>. Cultures were resuspended in the appropriate N-minimal medium with 2 mM sodium salicylate where indicated and incubated for an additional 30 min at 37°C before cells were harvested for RNA purification studies. For the complementation of *slyA* with *slyA* or *rovA* in *trans*, overnight cultures were diluted to 0.05 OD<sub>600</sub> and grown for 2 h at 24°C before arabinose was added to a final concentration of 0.02% (wt/vol). Cultures were grown for an additional 6 h before harvesting RNA.

*Y. pseudotuberculosis* strains YPIII and YP107 were diluted from overnight cultures to 0.05 OD<sub>600</sub> in LB and grown with shaking at 24°C. For the inhibition of H-NS via H-NST<sub>EPEC</sub> overexpression, and complementation of *rovA* with *rovA* or *slyA* in *trans*, YPIII and YP107 cultures carrying either pBAD18 or pRW57 were grown for 2 h before arabinose was added to a final concentration of 0.02% (wt/vol). Cultures were grown for an additional 6 h before harvesting RNA. For *slyA/rovA* complementation studies, *rpoAYS* primers targeting *rpoA* were used as loading controls, as *rpoA* is sufficiently conserved between the two species as to allow use of the same primers. For *rovA* promoter allelic exchange analysis, *Y. pseudotuberculosis* IP32953 and YPTB007 ( $n = 3$ ) were grown at 26°C with aeration. After 15 h, bacterial concentrations were determined by spectrophotometry and diluted to 0.1 OD<sub>600</sub> in fresh medium. Cultures were grown for 6 h at 26°C before cells were harvested for mRNA extraction. *rovA* and *inv* transcript levels were determined by qRT-PCR using Sybr Green and normalized to *gyrB* transcript levels (73, 74).

**NMR analysis of SlyA-salicylate.** SlyA protein for NMR analysis was prepared as an N-terminal 6 $\times$ His-tagged protein from cells grown in M9 minimal medium supplemented with <sup>15</sup>N-ammonium chloride (Cambridge Isotope Labs, Tewksbury, MA). SlyA protein expression was induced by the addition of 2 mM IPTG (isopropyl- $\beta$ -D-thiogalactopyranoside), and the protein was purified to homogeneity using Ni-affinity chromatography as previously described (21), except that samples were dialyzed in 50 mM Tris-HCl, pH 8.0, 150 mM NaCl, 0.1 mM EDTA, and 3 mM DTT following purification. Protein and ligand solutions for NMR experiments were prepared in 25 mM sodium phosphate, 150 mM NaCl buffer at pH 7.0 containing 10% D<sub>2</sub>O. NMR spectra were collected on a Bruker DMX 500-Mhz spectrometer (Bruker, Billerica, MA) on samples equilibrated at 35°C and consisting of 250 to 350  $\mu$ M <sup>15</sup>N-labeled His-SlyA in the absence or presence of 2 mM sodium salicylate or 0.5 mM sodium benzoate. Spectra were processed using NMR-Pipe (75) and analyzed using NMR-View (76).

**SlyA-salicylate crystallization.** SlyA was overexpressed and purified for crystallization as previously described (21), except that samples were dialyzed in 50 mM Tris-HCl, pH 8.0, 150 mM NaCl, 0.1 mM EDTA, and 3 mM DTT following purification. Cryo I and II sparse matrix crystallization screens (Emerald Biosystems, Bainbridge Island, WA) were used to determine initial conditions for His-SlyA crystal formation by sitting-drop vapor diffusion in 24-well crystal trays. Equal volumes (4  $\mu$ l) of SlyA and crystallization solutions were mixed before plates were sealed and kept at room temperature. Crystals appeared within 4 to 7 days in 20% PEG 300, 10% glycerol, 0.1 M phosphate-citrate buffer, pH 4.2, 0.2 M ammonium sulfate (condition 14). Subsequent crystal growth was performed using lab-made 20% PEG 400, 10% glycerol, 0.1 M phosphate-citrate buffer, pH 4.2, and 0.2 M ammonium sulfate. Crystallization of SlyA with sodium salicylate was achieved by adding dilutions of a 2 M sodium salicylate aqueous stock solution to the protein-crystallization solution mixture. SlyA-salicylate crystals appeared within 7 to 10 days. A single crystal appeared at a concentration of 75 mM sodium salicylate and grew to a maximum size of 500  $\mu$ m by 300  $\mu$ m by 150  $\mu$ m (Fig. S4). This crystal was used for X-ray diffraction experiments.

The crystal was frozen at 100 K in its crystallization solution for diffraction data collection on GM/CA-CAT beamline 23-ID-D at the Advanced Photon Source. The space group for the crystals is P21212 with two SlyA molecules in the asymmetric unit. The diffraction data were processed with HKL2000 (77). Data set statistics are shown in Table S1A. The crystal structure of the salicylate complex of SlyA was solved using a model of a previously investigated structure of apo-SlyA (unpublished data). That apo-structure was solved using the molecular replacement program MOLREP (78) with a search model generated by applying Swiss-Model (79) and the SlyA amino acid sequence to PDB entry 2FBH (80). The structural model for the salicylate complex was refined using REFMAC-5 (81) in the CCP4 suite (82).  $R_{free}$

(83) was calculated using 5% of the data in the test set. A high-resolution limit of 2.3 Å was applied for the refinement, consistent with standards appropriate when the structure was solved. This is the resolution at which  $R_{\text{merge}}$  for the data set drops below 0.40. XtalView (84) and Coot (85) were used to examine sigma A weighted  $|F_o|-|F_c|$  and  $2|F_o|-|F_c|$  electron density maps (86). MOLSCRIPT (87) and Raster3D (88) were used to produce structural figures for this paper. Table S1B contains refinement statistics for the structure.

**Ligand binding assays.** To estimate the  $K_D$  of ligand binding to SlyA, the quenching of intrinsic tryptophan fluorescence in SlyA was measured in the presence of the aromatic carboxylate benzoate. Benzoate was selected for these experiments because (i)  $^1\text{H},^{15}\text{N}$ -TROSY NMR spectra show that binding of benzoate induces chemical shift perturbations similar to those observed with other aromatic carboxylates such as salicylate and (ii) inner filter effects during fluorescence measurements can be avoided since there is little overlap in the UV spectra of benzoate and SlyA, and an  $\lambda_{\text{ex}}$  of 290 nm can be used to stimulate intrinsic SlyA tryptophan fluorescence. Titrations were conducted starting with 0.2  $\mu\text{M}$  His-SlyA in 25 mM  $\text{NaPO}_4$ , 150 mM NaCl, pH 7.0, at 25°C followed by sequential additions from an identical sample containing 2 mM sodium benzoate. Emission spectra from 320 to 450 nm ( $\lambda_{\text{ex}} = 290$  nm) were collected from samples ranging in benzoate concentration from 0 to 200 mM, and the change in maximum intensity was plotted as a function of benzoate concentration. The data were fitted to a standard hyperbolic binding isotherm yielding a  $K_D$  of  $\sim 40$   $\mu\text{M}$ .

**DNase I footprinting and DDFA.** DNase I footprinting was performed using methods described previously (1). SlyA was incubated at a final concentration of 2  $\mu\text{M}$  in the presence or absence of sodium salicylate with the target plasmid pRW39 for 10 min at 37°C. DNase I was added and allowed to digest the SlyA-DNA complex for 2 min at 37°C before the reaction mixture was quenched with cold stop buffer, purified, amplified by fluorescent primer extension using oligonucleotide 6-FAM-ydhI-R, and analyzed by differential DNA footprinting analysis (DDFA).

**6 $\times$ His-RovA purification.** RovA was purified using the same protocol as described previously for SlyA (17). However, overexpression cultures were grown at 24°C to an  $\text{OD}_{600}$  of 0.5. IPTG was added to a final concentration of 1 mM, cultures were incubated at 24°C for an additional 4 h before the cells were harvested by centrifugation, and cell pellets were stored at  $-80^\circ\text{C}$  for the subsequent purification of RovA.

**Western blot analysis.** For Western blot analyses, 1.0  $\text{OD}_{600}$  equivalent of total bacteria was harvested and lysed in SDS protein loading buffer. Equivalent amounts of 0.1 or 0.2  $\text{OD}_{600}$  were separated by SDS-PAGE and transferred to PVDF, and Western blotting was performed with rabbit anti-RovA antibody (1:1,000) (40).

**Data availability.** Coordinates and structure factors have been deposited in the Protein Data Bank with identifier 3DEU.

## SUPPLEMENTAL MATERIAL

Supplemental material for this article may be found at <https://doi.org/10.1128/mBio.00009-19>.

**FIG S1**, TIF file, 0.6 MB.

**FIG S2**, EPS file, 0.3 MB.

**FIG S3**, EPS file, 1.3 MB.

**FIG S4**, EPS file, 0.6 MB.

**TABLE S1**, DOCX file, 0.01 MB.

**TABLE S2**, DOCX file, 0.01 MB.

**TABLE S3**, DOCX file, 0.02 MB.

**TABLE S4**, DOCX file, 0.01 MB.

## ACKNOWLEDGMENTS

The National Institutes of Health provided support to F.C.F. (AI39557, AI44486, AI118962, and AI112640) and S.J.L. (A148622). GM/CA@APS has been funded in whole or in part with federal funds from the National Cancer Institute (ACB-12002) and the National Institute of General Medical Sciences (AGM-12006). This research used resources of the Advanced Photon Source, a U.S. Department of Energy (DOE) Office of Science User Facility operated for the DOE Office of Science by Argonne National Laboratory under contract no. DE-AC02-06CH11357.

We thank Eric Larson for helpful discussions and suggestions. We also thank Catherine Eakin and Ponni Rajagopal for assistance with protein purification and crystal growth, Petra Dersch for kindly providing *Y. pseudotuberculosis* YPIII and YP107, and Ralph Isberg for providing *Y. pseudotuberculosis* IP32953. Finally, we thank Rachel Kleivit for use of her NMR facilities to collect spectra of SlyA-salicylate complexes.

## REFERENCES

- Fang FC, Frawley ER, Tapscott T, Vázquez-Torres A. 2016. Discrimination and integration of stress signals by pathogenic bacteria. *Cell Host Microbe* 20:144–153. <https://doi.org/10.1016/j.chom.2016.07.010>.
- Ohno S. 1970. Evolution by gene duplication. Springer, New York, NY.
- Brenner SE, Hubbard T, Murzin A, Chothia C. 1995. Gene duplications in *H. influenzae*. *Nature* 378:140. <https://doi.org/10.1038/378140a0>.
- Teichmann SA, Park J, Chothia C. 1998. Structural assignments to the *Mycoplasma genitalium* proteins show extensive gene duplications and domain rearrangements. *Proc Natl Acad Sci U S A* 95:14658–14663.
- Teichmann SA, Babu MM. 2004. Gene regulatory network growth by duplication. *Nat Genet* 36:492–496. <https://doi.org/10.1038/ng1340>.
- Pérez-Rueda E, Collado-Vides J, Segovia L. 2004. Phylogenetic distribution of DNA-binding transcription factors in bacteria and archaea. *Comput Biol Chem* 28:341–350. <https://doi.org/10.1016/j.compbiolchem.2004.09.004>.
- Grove A. 2017. Regulation of metabolic pathways by MarR family transcription factors. *Comput Struct Biotechnol J* 15:366–371. <https://doi.org/10.1016/j.csbj.2017.06.001>.
- Alekshun MN, Levy SB, Mealy TR, Seaton BA, Head JF. 2001. The crystal structure of MarR, a regulator of multiple antibiotic resistance, at 2.3 Å resolution. *Nat Struct Biol* 8:710–714. <https://doi.org/10.1038/90429>.
- Seoane AS, Levy SB. 1995. Characterization of MarR, the repressor of the multiple antibiotic resistance (*mar*) operon in *Escherichia coli*. *J Bacteriol* 177:3414–3419. <https://doi.org/10.1128/jb.177.12.3414-3419.1995>.
- Martin RG, Rosner JL. 1995. Binding of purified multiple antibiotic-resistance repressor protein (MarR) to *mar* operator sequences. *Proc Natl Acad Sci U S A* 92:5456–5460. <https://doi.org/10.1073/pnas.92.12.5456>.
- George AM, Levy SB. 1983. Amplifiable resistance to tetracycline, chloramphenicol, and other antibiotics in *Escherichia coli*: involvement of a non-plasmid-determined efflux of tetracycline. *J Bacteriol* 155:531–540.
- Cohen SP, Levy SB, Foulds J, Rosner JL. 1993. Salicylate induction of antibiotic resistance in *Escherichia coli*: activation of the *mar* operon and a *mar*-independent pathway. *J Bacteriol* 175:7856–7862. <https://doi.org/10.1128/jb.175.24.7856-7862.1993>.
- Wilkinson SP, Grove A. 2006. Ligand-responsive transcriptional regulation by members of the MarR family of winged helix proteins. *Curr Issues Mol Biol* 8:51–62.
- Alekshun MN, Levy SB. 1999. The *mar* regulon: multiple resistance to antibiotics and other toxic chemicals. *Trends Microbiol* 7:410–413. [https://doi.org/10.1016/S0966-842X\(99\)01589-9](https://doi.org/10.1016/S0966-842X(99)01589-9).
- Hao Z, Lou H, Zhu R, Zhu J, Zhang D, Zhao BS, Zeng S, Chen X, Chan J, He C, Chen PR. 2014. The multiple antibiotic resistance regulator MarR is a copper sensor in *Escherichia coli*. *Nat Chem Biol* 10:21–28. <https://doi.org/10.1038/nchembio.1380>.
- Zhu R, Hao Z, Lou H, Song Y, Zhao J, Chen Y, Zhu J, Chen PR. 2017. Structural characterization of the DNA-binding mechanism underlying the copper(II)-sensing MarR transcriptional regulator. *J Biol Inorg Chem* 22:685–693. <https://doi.org/10.1007/s00775-017-1442-7>.
- Will WR, Bale DH, Reid PJ, Libby SJ, Fang FC. 2014. Evolutionary expansion of a regulatory network by counter-silencing. *Nat Commun* 5:5270. <https://doi.org/10.1038/ncomms6270>.
- Will WR, Navarre WW, Fang FC. 2015. Integrated circuits: how transcriptional silencing and counter-silencing facilitate bacterial evolution. *Curr Opin Microbiol* 23:8–13. <https://doi.org/10.1016/j.mib.2014.10.005>.
- Lithgow JK, Haider F, Roberts IS, Green J. 2007. Alternate SlyA and H-NS nucleoprotein complexes control *hlyE* expression in *Escherichia coli* K-12. *Mol Microbiol* 66:685–698. <https://doi.org/10.1111/j.1365-2958.2007.05950.x>.
- Perez JC, Latifi T, Groisman EA. 2008. Overcoming H-NS-mediated transcriptional silencing of horizontally acquired genes by the PhoP and SlyA proteins in *Salmonella enterica*. *J Biol Chem* 283:10773–10783. <https://doi.org/10.1074/jbc.M709843200>.
- Navarre WW, Halsey TA, Walthers D, Frye J, McClelland M, Potter JL, Kenney LJ, Gunn JS, Fang FC, Libby SJ. 2005. Co-regulation of *Salmonella enterica* genes required for virulence and resistance to antimicrobial peptides by SlyA and PhoP/PhoQ. *Mol Microbiol* 56:492–508. <https://doi.org/10.1111/j.1365-2958.2005.04553.x>.
- García Vescovi E, Soncini FC, Groisman EA. 1996. Mg<sup>2+</sup> as an extracellular signal: environmental regulation of *Salmonella* virulence. *Cell* 84:165–174. [https://doi.org/10.1016/S0092-8674\(00\)81003-X](https://doi.org/10.1016/S0092-8674(00)81003-X).
- Prost LR, Daley ME, Le Sage V, Bader MW, Le Moual H, Klevit RE, Miller SI. 2007. Activation of the bacterial sensor kinase PhoQ by acidic pH. *Mol Cell* 26:165–174. <https://doi.org/10.1016/j.molcel.2007.03.008>.
- Bader MW, Sanowar S, Daley ME, Schneider AR, Cho U, Xu W, Klevit RE, Le Moual H, Miller SI. 2005. Recognition of antimicrobial peptides by a bacterial sensor kinase. *Cell* 122:461–472. <https://doi.org/10.1016/j.cell.2005.05.030>.
- Thomson NR, Cox A, Bycroft BW, Stewart GS, Williams P, Salmond GP. 1997. The *rap* and *hor* proteins of *Erwinia*, *Serratia* and *Yersinia*: a novel subgroup in a growing superfamily of proteins regulating diverse physiological processes in bacterial pathogens. *Mol Microbiol* 26:531–544. <https://doi.org/10.1046/j.1365-2958.1997.5981976.x>.
- Dale C, Maudlin I. 1999. *Sodalis* gen. nov. and *Sodalis glossinidius* sp. nov., a microaerophilic secondary endosymbiont of the tsetse fly *Glossina morsitans morsitans*. *Int J Syst Bacteriol* 49:267–275. <https://doi.org/10.1099/00207713-49-1-267>.
- Akman L, Rio RV, Beard CB, Aksoy S. 2001. Genome size determination and coding capacity of *Sodalis glossinidius*, an enteric symbiont of tsetse flies, as revealed by hybridization to *Escherichia coli* gene arrays. *J Bacteriol* 183:4517–4525. <https://doi.org/10.1128/JB.183.15.4517-4525.2001>.
- Cathelyn JS, Crosby SD, Lathem WW, Goldman WE, Miller VL. 2006. RovA, a global regulator of *Yersinia pestis*, specifically required for bubonic plague. *Proc Natl Acad Sci U S A* 103:13514–13519. <https://doi.org/10.1073/pnas.0603456103>.
- Cathelyn JS, Ellison DW, Hinchliffe SJ, Wren BW, Miller VL. 2007. The RovA regulons of *Yersinia enterocolitica* and *Yersinia pestis* are distinct: evidence that many RovA-regulated genes were acquired more recently than the core genome. *Mol Microbiol* 66:189–205. <https://doi.org/10.1111/j.1365-2958.2007.05907.x>.
- Heroven AK, Nagel G, Tran HJ, Parr S, Dersch P. 2004. RovA is autoregulated and antagonizes H-NS-mediated silencing of *invasin* and *rovA* expression in *Yersinia pseudotuberculosis*. *Mol Microbiol* 53:871–888. <https://doi.org/10.1111/j.1365-2958.2004.04162.x>.
- Haque MM, Kabir MS, Aini LQ, Hirata H, Tsuyumu S. 2009. SlyA, a MarR family transcriptional regulator, is essential for virulence in *Dickeya dadantii* 3937. *J Bacteriol* 191:5409–5418. <https://doi.org/10.1128/JB.00240-09>.
- Weatherspoon-Griffin N, Wing HJ. 2016. Characterization of SlyA in *Shigella flexneri* identifies a novel role in virulence. *Infect Immun* 84:1073–1082. <https://doi.org/10.1128/IAI.00806-15>.
- Dolan KT, Duguid EM, He C. 2011. Crystal structures of SlyA protein, a master virulence regulator of *Salmonella*, in free and DNA-bound states. *J Biol Chem* 286:22178–22185. <https://doi.org/10.1074/jbc.M111.245258>.
- Curran TD, Abacha F, Hibberd SP, Rolfe MD, Lacey MM, Green J. 2017. Identification of new members of the *Escherichia coli* K-12 MG1655 SlyA regulon. *Microbiology* 163:400–409. <https://doi.org/10.1099/mic.0.000423>.
- Gama-Castro S, Salgado H, Santos-Zavaleta A, Ledezma-Tejeda D, Muñoz-Rascado L, García-Sotelo JS, Alquicira-Hernández K, Martínez-Flores I, Pannier L, Castro-Mondragón JA, Medina-Rivera A, Solano-Lira H, Bonavides-Martínez C, Pérez-Rueda E, Alquicira-Hernández S, Porrón-Sotelo L, López-Fuentes A, Hernández-Koutoucheva A, Del Moral-Chávez V, Rinaldi F, Collado-Vides J. 2016. RegulonDB version 9.0: high-level integration of gene regulation, coexpression, motif clustering and beyond. *Nucleic Acids Res* 44:D133–D143. <https://doi.org/10.1093/nar/gkv1156>.
- Perera IC, Grove A. 2010. Molecular mechanisms of ligand-mediated attenuation of DNA binding by MarR family transcriptional regulators. *J Mol Cell Biol* 2:243–254. <https://doi.org/10.1093/jmcb/mjq021>.
- Octavia S, Lan R. 2014. The family *Enterobacteriaceae*, p 225–286. In Rosenberg E, DeLong EF, Lory S, Stackebrandt E, Thompson F (ed), *The prokaryotes: gammaproteobacteria*. Springer, Berlin, Germany.
- Lomovskaya O, Lewis K. 1992. Emr, an *Escherichia coli* locus for multidrug resistance. *Proc Natl Acad Sci U S A* 89:8938–8942. <https://doi.org/10.1073/pnas.89.19.8938>.
- Lomovskaya O, Lewis K, Matin A. 1995. EmrR is a negative regulator of the *Escherichia coli* multidrug resistance pump EmrAB. *J Bacteriol* 177:2328–2334. <https://doi.org/10.1128/jb.177.9.2328-2334.1995>.
- Ellison DW, Miller VL. 2006. H-NS represses *inv* transcription in *Yersinia*

- enterocolitica* through competition with RovA and interaction with YmoA. *J Bacteriol* 188:5101–5112. <https://doi.org/10.1128/JB.00862-05>.
41. Revell PA, Miller VL. 2000. A chromosomally encoded regulator is required for expression of the *Yersinia enterocolitica* *inv* gene and for virulence. *Mol Microbiol* 35:677–685.
  42. Tran HJ, Heroven AK, Winkler L, Spreter T, Beatrix B, Dersch P. 2005. Analysis of RovA, a transcriptional regulator of *Yersinia pseudotuberculosis* virulence that acts through antirepression and direct transcriptional activation. *J Biol Chem* 280:42423–42432. <https://doi.org/10.1074/jbc.M504464200>.
  43. Shi X, Bennett GN. 1994. Plasmids bearing *hfq* and the *hns*-like gene *stpA* complement *hns* mutants in modulating arginine decarboxylase gene expression in *Escherichia coli*. *J Bacteriol* 176:6769–6775. <https://doi.org/10.1128/jb.176.21.6769-6775.1994>.
  44. Sonden B, Uhlin BE. 1996. Coordinated and differential expression of histone-like proteins in *Escherichia coli*: regulation and function of the H-NS analog StpA. *EMBO J* 15:4970–4980. <https://doi.org/10.1002/j.1460-2075.1996.tb00877.x>.
  45. Williamson HS, Free A. 2005. A truncated H-NS-like protein from enteropathogenic *Escherichia coli* acts as an H-NS antagonist. *Mol Microbiol* 55:808–827. <https://doi.org/10.1111/j.1365-2958.2004.04421.x>.
  46. McVicker G, Sun L, Sohanpal BK, Gashi K, Williamson RA, Plumbridge J, Blomfield IC. 2011. SlyA protein activates *fimB* gene expression and type 1 fimbriation in *Escherichia coli* K-12. *J Biol Chem* 286:32026–32035. <https://doi.org/10.1074/jbc.M111.266619>.
  47. Wyborn NR, Stapleton MR, Norte VA, Roberts RE, Grafton J, Green J. 2004. Regulation of *Escherichia coli* hemolysin E expression by H-NS and *Salmonella* SlyA. *J Bacteriol* 186:1620–1628. <https://doi.org/10.1128/JB.186.6.1620-1628.2004>.
  48. Corbett D, Bennett HJ, Askar H, Green J, Roberts IS. 2007. SlyA and H-NS regulate transcription of the *Escherichia coli* K5 capsule gene cluster, and expression of *slyA* in *Escherichia coli* is temperature-dependent, positively autoregulated, and independent of H-NS. *J Biol Chem* 282:33326–33335. <https://doi.org/10.1074/jbc.M703465200>.
  49. Saridakis V, Shahinas D, Xu X, Christendat D. 2008. Structural insight on the mechanism of regulation of the MarR family of proteins: high-resolution crystal structure of a transcriptional repressor from *Methanobacterium thermoautotrophicum*. *J Mol Biol* 377:655–667. <https://doi.org/10.1016/j.jmb.2008.01.001>.
  50. Hong M, Fuangthong M, Helmann JD, Brennan RG. 2005. Structure of an OhrR-*ohrA* operator complex reveals the DNA binding mechanism of the MarR family. *Mol Cell* 20:131–141. <https://doi.org/10.1016/j.molcel.2005.09.013>.
  51. Sabater-Muñoz B, Toft C, Alvarez-Ponce D, Fares MA. 2017. Chance and necessity in the genome evolution of endosymbiotic bacteria of insects. *ISME J* 11:1291–1304. <https://doi.org/10.1038/ismej.2017.18>.
  52. Zou L, Zeng Q, Lin H, Gyaneshwar P, Chen G, Yang CH. 2012. SlyA regulates type III secretion system (T3SS) genes in parallel with the T3SS master regulator HrpL in *Dickeya dadantii* 3937. *Appl Environ Microbiol* 78:2888–2895. <https://doi.org/10.1128/AEM.07021-11>.
  53. Nicholson R, Hammerschmidt R. 1992. Phenolic-compounds and their role in disease resistance. *Annu Rev Phytopathol* 30:369–389. <https://doi.org/10.1146/annurev.py.30.090192.002101>.
  54. Salgado H, Peralta-Gil M, Gama-Castro S, Santos-Zavaleta A, Muñoz-Rascado L, García-Sotelo JS, Weiss V, Solano-Lira H, Martínez-Flores I, Medina-Rivera A, Salgado-Osorio G, Alquicira-Hernández S, Alquicira-Hernández K, López-Fuentes A, Porrón-Sotelo L, Huerta AM, Bonavides-Martínez C, Balderas-Martínez YI, Pannier L, Olvera M, Labastida A, Jiménez-Jacinto V, Vega-Alvarado L, Del Moral-Chávez V, Hernández-Alvarez A, Morett E, Collado-Vides J. 2013. RegulonDB v8.0: omics data sets, evolutionary conservation, regulatory phrases, cross-validated gold standards and more. *Nucleic Acids Res* 41:D203–D213. <https://doi.org/10.1093/nar/gks1201>.
  55. Kröger C, Colgan A, Srikumar S, Händler K, Sivasankaran SK, Hammarlöf DL, Canals R, Grissom JE, Conway T, Hokamp K, Hinton JC. 2013. An infection-relevant transcriptomic compendium for *Salmonella enterica* serovar Typhimurium. *Cell Host Microbe* 14:683–695. <https://doi.org/10.1016/j.chom.2013.11.010>.
  56. Lawrenz MB, Miller VL. 2007. Comparative analysis of the regulation of *rovA* from the pathogenic yersiniae. *J Bacteriol* 189:5963–5975. <https://doi.org/10.1128/JB.00528-07>.
  57. Thomason MK, Bischler T, Eisenbart SK, Förstner KU, Zhang A, Herbig A, Nieselt K, Sharma CM, Storz G. 2015. Global transcriptional start site mapping using differential RNA sequencing reveals novel antisense RNAs in *Escherichia coli*. *J Bacteriol* 197:18–28. <https://doi.org/10.1128/JB.02096-14>.
  58. Osborne SE, Walthers D, Tomljenovic AM, Mulder DT, Silphaduang U, Duong N, Lowden MJ, Wickham ME, Waller RF, Kenney LJ, Coombes BK. 2009. Pathogenic adaptation of intracellular bacteria by rewiring a *cis*-regulatory input function. *Proc Natl Acad Sci U S A* 106:3982–3987. <https://doi.org/10.1073/pnas.0811669106>.
  59. Bölin I, Norlander L, Wolf-Watz H. 1982. Temperature-inducible outer membrane protein of *Yersinia pseudotuberculosis* and *Yersinia enterocolitica* is associated with the virulence plasmid. *Infect Immun* 37:506–512.
  60. Quade N, Mendonca C, Herbst K, Heroven AK, Ritter C, Heinz DW, Dersch P. 2012. Structural basis for intrinsic thermosensing by the master virulence regulator RovA of *Yersinia*. *J Biol Chem* 287:35796–35803. <https://doi.org/10.1074/jbc.M112.379156>.
  61. Datsenko KA, Wanner BL. 2000. One-step inactivation of chromosomal genes in *Escherichia coli* K-12 using PCR products. *Proc Natl Acad Sci U S A* 97:6640–6645. <https://doi.org/10.1073/pnas.120163297>.
  62. Stringer AM, Singh N, Yermakova A, Petrone BL, Amarasinghe JJ, Reyes-Diaz L, Mantis NJ, Wade JT. 2012. FRUIT, a scar-free system for targeted chromosomal mutagenesis, epitope tagging, and promoter replacement in *Escherichia coli* and *Salmonella enterica*. *PLoS One* 7:e44841. <https://doi.org/10.1371/journal.pone.0044841>.
  63. Kingsley RA, Reissbrodt R, Rabsch W, Ketley JM, Tsois RM, Everest P, Dougan G, Bäuml AJ, Roberts M, Williams PH. 1999. Ferrioxamine-mediated iron(III) utilization by *Salmonella enterica*. *Appl Environ Microbiol* 65:1610–1618.
  64. de Lorenzo V, Cases I, Herrero M, Timmis KN. 1993. Early and late responses of TOL promoters to pathway inducers: identification of post-exponential promoters in *Pseudomonas putida* with *lacZ-tet* bicistronic reporters. *J Bacteriol* 175:6902–6907. <https://doi.org/10.1128/jb.175.21.6902-6907.1993>.
  65. Lopez CA, Winter SE, Rivera-Chávez F, Xavier MN, Poon V, Nuccio SP, Tsois RM, Bäuml AJ. 2012. Phage-mediated acquisition of a type III secreted effector protein boosts growth of *Salmonella* by nitrate respiration. *mBio* 3:e00143-12. <https://doi.org/10.1128/mBio.00143-12>.
  66. Chain PS, Carniel E, Larimer FW, Lamerdin J, Stoutland PO, Regala WM, Georgescu AM, Vergez LM, Land ML, Motin VL, Brubaker RR, Fowler J, Hinnebusch J, Marceau M, Medigue C, Simonet M, Chenal-Francisque V, Souza B, Dacheux D, Elliott JM, Derbise A, Hauser LJ, Garcia E. 2004. Insights into the evolution of *Yersinia pestis* through whole-genome comparison with *Yersinia pseudotuberculosis*. *Proc Natl Acad Sci U S A* 101:13826–13831. <https://doi.org/10.1073/pnas.0404012101>.
  67. Merriam JJ, Mathur R, Maxfield-Boumil R, Isberg RR. 1997. Analysis of the *Legionella pneumophila* *flil* gene: intracellular growth of a defined mutant defective for flagellum biosynthesis. *Infect Immun* 65:2497–2501.
  68. Wang RF, Kushner SR. 1991. Construction of versatile low-copy-number vectors for cloning, sequencing and gene expression in *Escherichia coli*. *Gene* 100:195–199. [https://doi.org/10.1016/0378-1119\(91\)90366-J](https://doi.org/10.1016/0378-1119(91)90366-J).
  69. Guzman LM, Belin D, Carson MJ, Beckwith J. 1995. Tight regulation, modulation, and high-level expression by vectors containing the arabinose  $P_{BAD}$  promoter. *J Bacteriol* 177:4121–4130. <https://doi.org/10.1128/jb.177.14.4121-4130.1995>.
  70. Amann E, Ochs B, Abel KJ. 1988. Tightly regulated *tac* promoter vectors useful for the expression of unfused and fused proteins in *Escherichia coli*. *Gene* 69:301–315. [https://doi.org/10.1016/0378-1119\(88\)90440-4](https://doi.org/10.1016/0378-1119(88)90440-4).
  71. Hashimoto-Gotoh T, Yamaguchi M, Yasojima K, Tsujimura A, Wakabayashi Y, Watanabe Y. 2000. A set of temperature sensitive-replication/-segregation and temperature resistant plasmid vectors with different copy numbers and in an isogenic background (chloramphenicol, kanamycin, *lacZ*, *repA*, *par*, *polA*). *Gene* 241:185–191. [https://doi.org/10.1016/S0378-1119\(99\)00434-5](https://doi.org/10.1016/S0378-1119(99)00434-5).
  72. Aparicio O, Geisberg JV, Sekinger E, Yang A, Moqtaderi Z, Struhl K. 2005. Chromatin immunoprecipitation for determining the association of proteins with specific genomic sequences *in vivo*. *Curr Protoc Mol Biol* Chapter 21:Unit 21.3. <https://doi.org/10.1002/0471142727.mb2103s69>.
  73. Lawrenz MB, Lenz JD, Miller VL. 2009. A novel autotransporter adhesin is required for efficient colonization during bubonic plague. *Infect Immun* 77:317–326. <https://doi.org/10.1128/IAI.01206-08>.
  74. Lenz JD, Lawrenz MB, Cotter DG, Lane MC, Gonzalez RJ, Palacios M, Miller VL. 2011. Expression during host infection and localization of *Yersinia pestis* autotransporter proteins. *J Bacteriol* 193:5936–5949. <https://doi.org/10.1128/JB.05877-11>.
  75. Delaglio F, Grzesiek S, Vuister GW, Zhu G, Pfeifer J, Bax A. 1995. NMRPipe:

- a multidimensional spectral processing system based on UNIX pipes. *J Biomol NMR* 6:277–293.
76. Johnson BA, Blevins RA. 1994. NMR View: a computer program for the visualization and analysis of NMR data. *J Biomol NMR* 4:603–614. <https://doi.org/10.1007/BF00404272>.
  77. Otwinowski Z, Minor W. 1997. Processing of X-ray diffraction data collected in oscillation mode. *Methods Enzymol* 276:307–326. [https://doi.org/10.1016/S0076-6879\(97\)76066-X](https://doi.org/10.1016/S0076-6879(97)76066-X).
  78. Vagin A, Teplyakov A. 1997. *MOLREP*: an automated program for molecular replacement. *J Appl Crystallogr* 30:1022–1025. <https://doi.org/10.1107/S0021889897006766>.
  79. Schwede T, Kopp J, Guex N, Peitsch MC. 2003. SWISS-MODEL: an automated protein homology-modeling server. *Nucleic Acids Res* 31:3381–3385. <https://doi.org/10.1093/nar/gkg520>.
  80. Lunin V, Evdokimova E, Kudritska M, Osipiuk J, Joachimiak A, Edwards A, Savchenko A, Midwest Center for Structural Genomics. 2005. The crystal structure of transcriptional regulator PA3341. RCSB PDB accession no. 2FBH.
  81. Murshudov GN, Vagin AA, Dodson EJ. 1997. Refinement of macromolecular structures by the maximum-likelihood method. *Acta Crystallogr D Biol Crystallogr* 53:240–255. <https://doi.org/10.1107/S0907444996012255>.
  82. Collaborative Computational Project. 1994. The CCP4 suite: programs for protein crystallography. *Acta Crystallogr D Biol Crystallogr* 50:760–763. <https://doi.org/10.1107/S0907444994003112>.
  83. Brünger AT. 1993. Assessment of phase accuracy by cross validation: the free R value. *Methods and applications. Acta Crystallogr D Biol Crystallogr* 49:24–36. <https://doi.org/10.1107/S0907444992007352>.
  84. McRee DE. 1999. XtalView/Xfit—a versatile program for manipulating atomic coordinates and electron density. *J Struct Biol* 125:156–165. <https://doi.org/10.1006/jsbi.1999.4094>.
  85. Emsley P, Cowtan K. 2004. Coot: model-building tools for molecular graphics. *Acta Crystallogr D Biol Crystallogr* 60:2126–2132. <https://doi.org/10.1107/S0907444904019158>.
  86. Read RJ. 1986. Improved Fourier coefficients for maps using phases from partial structures with errors. *Acta Crystallogr A Found Crystallogr* 42:140–149. <https://doi.org/10.1107/S0108767386099622>.
  87. Kraulis P. 1991. MOLSCRIPT: a program to produce both detailed and schematic plots of protein structures. *J Appl Crystallogr* 24:946–950. <https://doi.org/10.1107/S0021889891004399>.
  88. Merritt EA, Bacon DJ. 1997. Raster3D: photorealistic molecular graphics. *Methods Enzymol* 277:505–524. [https://doi.org/10.1016/S0076-6879\(97\)77028-9](https://doi.org/10.1016/S0076-6879(97)77028-9).
  89. Le SQ, Gascuel O. 2008. An improved general amino acid replacement matrix. *Mol Biol Evol* 25:1307–1320. <https://doi.org/10.1093/molbev/msn067>.
  90. Kumar S, Stecher G, Li M, Knyaz C, Tamura K. 2018. MEGA X: molecular evolutionary genetics analysis across computing platforms. *Mol Biol Evol* 35:1547–1549. <https://doi.org/10.1093/molbev/msy096>.
  91. Di Tommaso P, Moretti S, Xenarios I, Orobitt M, Montanyola A, Chang JM, Taly JF, Notredame C. 2011. T-Coffee: a web server for the multiple sequence alignment of protein and RNA sequences using structural information and homology extension. *Nucleic Acids Res* 39:W13–W17. <https://doi.org/10.1093/nar/gkr245>.
  92. Caspi R, Billington R, Ferrer L, Foerster H, Fulcher CA, Keseler IM, Kothari A, Krummenacker M, Latendresse M, Mueller LA, Ong Q, Paley S, Subhraveti P, Weaver DS, Karp PD. 2016. The MetaCyc database of metabolic pathways and enzymes and the BioCyc collection of pathway/genome databases. *Nucleic Acids Res* 44:D471–D480. <https://doi.org/10.1093/nar/gkv1164>.
  93. Tamura K, Nei M. 1993. Estimation of the number of nucleotide substitutions in the control region of mitochondrial DNA in humans and chimpanzees. *Mol Biol Evol* 10:512–526. <https://doi.org/10.1093/oxfordjournals.molbev.a040023>.